



## Review

# Principles of demineralization: Modern strategies for the isolation of organic frameworks

## Part II. Decalcification

Hermann Ehrlich<sup>a,\*</sup>, Petros G. Koutsoukos<sup>b</sup>, Konstantinos D. Demadis<sup>c</sup>, Oleg S. Pokrovsky<sup>d</sup>

<sup>a</sup> Max Bergmann Center of Biomaterials, Institute of Materials Science, Dresden University of Technology, Budapester Str. 27, D-01069 Dresden, Germany

<sup>b</sup> Laboratory of Inorganic and Analytical Chemistry, Department of Chemical Engineering, University of Patras, GR-265 04 Patras, Greece

<sup>c</sup> Crystal Engineering, Growth and Design Laboratory, Department of Chemistry, University of Crete, Voutes Campus, GR-71003 Heraklion, Crete, Greece

<sup>d</sup> Laboratory of Mechanisms and Transfer in Geology, Observatory Midi-Pyrenees (OMP), UMR 5563, CNRS, 14 Avenue Edouard Belin, 31400 Toulouse, France

## ARTICLE INFO

## Article history:

Received 8 May 2008

Accepted 30 June 2008

## Keywords:

Biomaterialization

Demineralization

Decalcification

Mechanisms

Calcium release

Bioerosion

Dissolution

## ABSTRACT

This is the second paper on principles of demineralization. The initial paper is dedicated to the common definitions and the history of demineralization. In present work we review the principles and mechanisms of decalcification, i.e., removing the mineral Ca-containing compounds (phosphates and carbonates) from the organic matrix in its two main aspects: natural and artificial. Natural chemical erosion of biominerals (cavitation of biogenic calcareous substrata by bacteria, fungi, algae, foraminifera, sponges, polychaetes, and mollusks) is driven by production of mineral and organic acids, acidic polysaccharides, and enzymes (carbonic anhydrase, alkaline and phosphoprotein phosphatases, and H<sup>+</sup>-ATPase). Examples of artificial decalcification includes demineralization of bone, dentin and enamel, and skeletal formations of corals and crustacean. The mechanism and kinetics of Ca-containing biomineral dissolution is analyzed within the framework of (i) diffusion-reaction theory; (ii) surface-reaction controlled, morphology-based theories, and (iii) phenomenological surface coordination models. The application of surface complexation model for describing and predicting the effect of organic ligands on calcium and magnesium dissolution kinetics is also described. Use of the electron microscopy-based methods for observation and visualization of the decalcification phenomenon is discussed.

© 2008 Elsevier Ltd. All rights reserved.

## Contents

1. Introduction . . . . .	170
2. Biological decalcification . . . . .	170
3. Enzymes and their role in decalcification. . . . .	173
3.1. Carbonic anhydrase (CA) . . . . .	173
3.2. Phosphoprotein phosphatase . . . . .	174
3.3. Vacuolar-type H <sup>+</sup> -ATPase . . . . .	174
4. Mechanisms and kinetics of the demineralization of Ca-containing biomaterials . . . . .	174
4.1. Calcium phosphates . . . . .	174
4.2. Mechanism and kinetics of the dissolution of Ca-containing biomaterials . . . . .	176
4.3. Models for the dissolution process . . . . .	176
4.3.1. Diffusion-reaction theory . . . . .	176
4.3.2. Surface-reaction controlled morphology-based theories . . . . .	177
4.3.3. Phenomenological surface coordination models: case studies of effect of organic ligands on calcium and magnesium carbonates dissolution. . . . .	179
5. Demineralization of naturally occurring Ca-containing biocomposites. . . . .	180
5.1. Bone . . . . .	180

\* Corresponding author.

E-mail address: [Hermann.ehrlich@tu-dresden.de](mailto:Hermann.ehrlich@tu-dresden.de) (H. Ehrlich).

5.2. Dentin and enamel.....	181
5.3. Corals.....	183
5.4. Crustacea.....	184
6. Epilogue.....	188
Acknowledgements.....	189
References.....	189

## 1. Introduction

Demineralization is the process of loss of the mineral phase of the hard tissues of living organisms. Hard tissues are composed of insoluble calcium salts of carbonate, silicate and phosphate ions. Organisms like fungi, algae and cyanobacteria encountered in aquatic systems are capable of growing on calcareous substrates which they dissolve possible through the development of a micro-environment in which the conditions (saturation) are favourable for the dissolution of calcium carbonate. On the other hand the role of microorganisms is known to be detrimental for the dissolution of the apatitic minerals present in tooth and bone. Calcium carbonate minerals may be encountered in nature in three different polymorphs in the order of decreasing solubility: vaterite, aragonite and calcite (Plummer and Busenberg, 1982; Kitano, 1962). The presence of these minerals depends on the chemistry of the environment in which they are formed and on factors such as the temperature of the aquatic environment and the presence of various foreign ions. Because of the fact that the three polymorphs of calcium carbonate have different arrangement of their constituent calcium and carbonate ions, their interaction and resistance to the activity of living organisms varies. The calcium phosphate phases found in hard tissues which include calcium phosphate dihydrate ( $\text{CaHPO}_4 \cdot 2\text{H}_2\text{O}$ , DCPD), octacalcium phosphate ( $\text{Ca}_8\text{H}_2(\text{PO}_4)_6 \cdot 5\text{H}_2\text{O}$ , OCP), tricalcium phosphate ( $\beta\text{-Ca}_3(\text{PO}_4)_2$ ,  $\beta\text{-TCP}$ ) and hydroxyapatite ( $\text{Ca}_5(\text{PO}_4)_3\text{OH}$ , HAP) make the demineralization picture complicated (Nancollas and Wu, 2000; Spanos et al., 2006a,b). HAP is the thermodynamically most stable phase of calcium phosphates and is the model inorganic compound for hard tissues (Ackerman et al., 1992). Besides the markedly different solubilities of these mineral phases, their stability may be significantly affected not only by the composition of the micro-environment in contact with the solid phase but also by the presence of various foreign compounds. Understanding thermodynamics and accurate measurements of the kinetics is needed for drawing mechanistic conclusions concerning demineralization. Both thermodynamics the kinetics of mineral dissolution during biological demineralization depend very much on the activity of micro-organisms and/or enzymes. It is important to note

that in the demineralization of tooth enamel, although the microbial film is necessary for the demineralization, it is not sufficient. This underlines the fact that the mechanism of biological demineralization is complex and efforts are needed towards obtaining a thorough understanding of the process. The principal task of this paper is to review the literature concerned with the mechanism of biological demineralization focusing both in biological and physico-chemical parameters associated with the process. This contribution is a follow-up of previous paper in which the principles of demineralization over very wide spectrum of disciplines were reviewed. In the present paper we have reviewed biological decalcification processes in aquatic environments mediated by micro-organisms and enzymic activity, involving the dissolution of calcitic substrates. Next, thermodynamics and kinetics based mechanistic analyses of the demineralization process are surveyed presenting the case of another important class of biominerals, calcium phosphates. This part of fundamentals is followed by the review of demineralization processes in the hard tissues of higher mammals, i.e. bone and teeth (dentin and enamel) and also demineralization involving calcium carbonate typically encountered in corals and crustacean. Different kinds of electron microscopy techniques and their use in investigations of decalcification phenomenon are discussed.

## 2. Biological decalcification

The phenomena of biological demineralization, including biologically induced decalcification, are widely distributed in nature. The *calcibiocavicole activity* (Carriker and Smith, 1969) is a fact well investigated and described for different unicellular and metazoan organisms. That the nature of the environment may be a factor in the development of the penetrating habit, is suggested by the fact that the great majority of calcibiocavicole species are marine (indeed, cariogenic microorganisms in oral cavities of vertebrates function in a “marine-like” environment). Grazing on surface biofilms by hard-toothed higher animals and invertebrates, as well as by the growth of chasmolitic and cryptoendolithic microbes can result in significant physical and chemical erosion of biominerals (Garcia-Pichel, 2006) (Fig. 1). Cavitation of biogenic calcareous

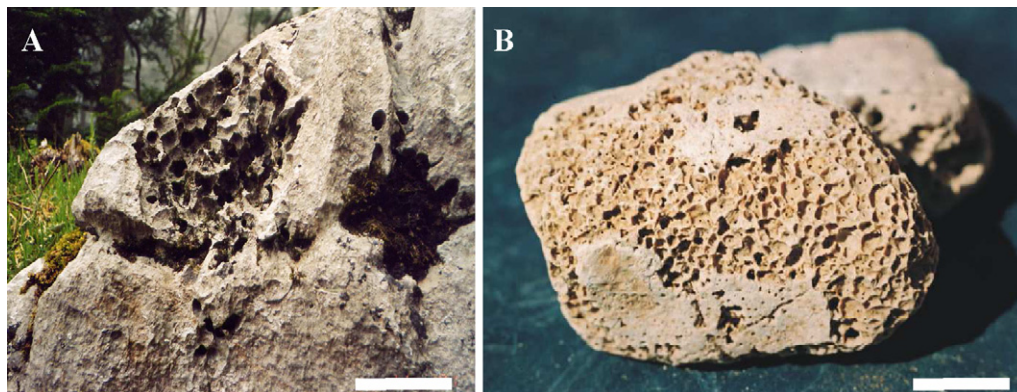
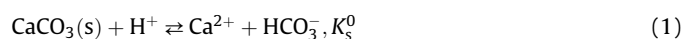


**Fig. 1.** Drilling traces performed by (A) snails boring into the limestone via exopolysaccharide/mineral acids excretions (bar 20 cm), and (B) by the boring sponge *Cliona vermifera* (image courtesy W.E.G. Müller, bar 0.5 cm).

substrata may provide bacteria, fungi, and algae with nutrients from the organic matrix which are not otherwise available (Carriker and Smith, 1969). Aerobic heterotrophic bacteria, fermenting, sulphide-oxidizing and nitrifying bacteria, can dissolve acid-labile minerals due to the production of acids as by-products of metabolism (carbonic, organic, sulphuric and nitric acids, respectively) (Ehrlich, 1996). Also lichens and fungi in soils produce organic acids such as lactic, succinic, oxalic, citric, acetic and  $\alpha$ -keto acids (reviewed in Kalinowski et al., 2000). These dissolved acids and other organic exudates can affect pH in weathering solutions and thereby promote or inhibit etching. Organic ligands can complex cations in solution, inhibit precipitation or lower the saturation index in solution and enhance dissolution indirectly. Simple and complex organic ligands are able to adsorb on the mineral surface and thus modify their dissolution rates via polarizing the metal–oxygen bonds or bridging several reactive surface centers together as described for the application to ligand-promoted or inhibited dissolution of carbonates (Pokrovsky and Schott, 2001; Jordan et al., 2007; Golubev et al., submitted), oxides (Pokrovsky et al., 2005) and silicates (Golubev et al., 2006; Golubev and Pokrovsky, 2006). Studies by Welsh and Vandevivere (1994) have also shown that insoluble extracellular polysaccharides can both increase or decrease dissolution of minerals under different conditions. Fungi, microalgae and cyanobacteria that actively dissolve carbonate substrates, excavate microscopic galleries as they grow within them. While the boring mechanism of any of these organisms remains unknown, the production of acid equivalents has often been suggested (Golubic et al., 1984).

Three alternative mechanistic models for better understanding of cyanobacterial boring mechanisms were recently proposed by Garcia-Pichel (2006). They are based on either temporal or spatial separation of photosynthesis and respiration, and on the active extrusion of calcium ions through an active cellular uptake and transport process. From the three models, the latter is shown to be most appropriate in describing and explaining the boring phenomenon. Briefly, the thermodynamic equilibrium for metal carbonate dissolution–precipitation is known as follow:



towards the solid phase. The free energy of dissolution is given by

$$\Delta G_{\text{diss}} = -R_g T \ln \frac{\text{IAP}}{K_s^0} \quad (2)$$

where  $R_g$  is the gas constant,  $T$  the absolute temperature, IAP the ion activity product and  $K_s^0$  is the thermodynamic solubility product of the respective salt (Stumm and Morgan, 1996). Dissolution of crystals present in solutions takes place provided that the condition  $\text{IAP} < K_s^0$  is met. In cyanobacteria, as in all organisms, intracellular calcium is tightly regulated at the cost of energy through independent processes of calcium uptake and efflux. The normal levels of intracellular calcium are maintained at about 0.1–0.2  $\mu\text{M}$ , to prevent toxicity to the cell metabolism, but transient levels may rise to 5  $\mu\text{M}$  in cyanobacteria (Torrecilla et al., 2001). If external  $\text{Ca}^{2+}$  concentrations exceed these concentration levels, as is typically the case, calcium uptake may involve low passive permeability and/or  $\text{Ca}^{2+}$ -sensitive trans-membrane channels. Efflux can be mediated by  $\text{Ca}^{2+}/\text{H}^+$  antiporters or by  $\text{Ca}^{2+}$ -ATPases, powered by proton motive force of energized membranes or by intracellular coupling with ATP hydrolysis, respectively. Thus, there is evidence for the presence of the building blocks needed for the calcium pump mechanism. Garcia-Pichel proposed a mechanism based on the active transport of  $\text{Ca}^{2+}$  through the cyanobacterial filament so that low concentration of free  $\text{Ca}^{2+}$  develop in the interstitial space at the end of the tunnel.

As a result, IAP values are reduced below levels that would favour thermodynamically the dissolution of the mineral phase. This model is consistent with the coincidence in microetching evidence found by Alexanderson (1975) and Fredd and Fogler (1998a,b), which points to a dissolution mode by cation removal in a similar way as the addition of chelators at high pH. Moreover, the model is consistent with the known range of bored substrates, which share only  $\text{Ca}^{2+}$  as the common ion constituent (as, for example, in hydroxyapatite and calcite). An additional feature of this model is that the problem of re-precipitation of carbonate is by-passed, because transport of the cation occurs intracellularly, effectively isolated from the interstitial space, where the local IAP would not be increased above the background levels, even though pH and  $\text{HCO}_3^-$  concentrations would (Garcia-Pichel, 2006).

A large variety of organic and inorganic substrates such as wood, mollusc shells, bryozoan skeletons, crustacean carapaces, corals have been found infested with boring foraminiferans (Venec-Peyre, 1996; Wisshak and Rüggeberg, 2006). They act as bioeroders of skeletal grains and contribute to the production of fine and very fine particles (Venec-Peyre, 1987). The Foraminifera represent one of the most ecologically important groups of marine heterotrophic protists, the evolutionary history of which is well known for biomineralized lineages, and many of these are key indices in biostratigraphic, paleoceanographic, and paleoclimatic reconstructions (Pawlowski et al., 2003).

Venec-Peyre (1987) suggests that the boring processes in case of Foraminifera are chemical in nature. Due to the unicellular nature of the borers, the relevant borings cannot result from the activity of differentiated organs (rasps or another adapted system) as with other borers. Regarding the perforated calcareous species, the protoplasm itself secretes calcium carbonate required for test elaboration. The cell probably acts by gradually and completely dissolving the substratum, resulting in the fragile looking aspects of the cavity outline, and by removal of ions. For agglutinated foraminiferan species, the process is somewhat different. The dissolution of the substrate seems to be incomplete and leads to the weakening of the carbonate framework into minute aggregates. The latter, as the various wastes on the surface of the substrate, are moved and accumulated near the Foraminifera by pseudopodia. Secondly, the aggregates are gathered on the organic lining and joined by a cement secreted by the cell. The purpose of such penetration may be to protect themselves against water turbulence and to provide material for test construction (Venec-Peyre, 1987).

Sponges (Porifera) are known as the first multicellular organisms in earth. Whereas many sponges are chemically or mechanically defended, some that have no such defences and may have the competitive advantage of using a substrate that other organisms cannot use. One such strategy is to bore into the carbonate substrate that is out of reach for most predators, with the additional advantage of using a space unavailable to their competitors (Zundevich et al., 2007). Thus, boring sponges (Fig. 1B), mostly from the family Clionidae, generally dominate the bioeroders community (Risk et al., 1995; Calcinaï et al., 2000). These sponges inhabit cavities which they excavate in coral, the valves of living molluscs, dead shells, and calcareous rock. During penetration the substrate is gradually destroyed as the sponge hollows out an extensive system of cavities and tunnels. Preliminary studies revealed that these excavations are produced as small fragments of calcareous material are removed by a special type of amoebocyte which exhibits an etching activity (Cobb, 1969). Cellular penetration occurs along the interface where these cells contact the substrate and is characterized by a unique pattern of cell–substrate relationships. Each active cell releases a substance which dissolves the substrate around its edge, forming

a linear etching which corresponds in size and shape to the contours of the cell. Deeper etching occurs at the cell edge, moving gradually downward through the initial etching, sinks into the substrate in a noose-like fashion. During this movement the cell border is drawn down through the slit-like crevice cut by the cell edge, while the nucleus remains in position on the surface of the substrate within the original etched outline. Eventually, the undercutting action is completed and a small chip is freed from the substrate. Thus, penetration is achieved by the precise cellular release of a chemical agent which dissolves the calcareous substrate along restricted zones of contact between cell and substrate (Cobb, 1969). Carbonic anhydrase and acid phosphatase are probably involved in this process (Pomponi, 1980).

Rates of bioerosion induced by sponges depend on several biotic and abiotic factors, including nutrient and food availability, temperature, physiological state of organism, density and type of substrate and the presence of etching occurs at the cell edge (Zundelevich et al., 2007; Schönberg, 2002a,b). Previously, Vacelet (1981) proposed that sponge zooxanthellae have an influence on the calcium carbonate solubility and a general stimulatory effect on the host metabolism. Recently, Schönberg (2006) showed that growth and erosion of the zooxanthellate Australian bioeroding sponge *Cliona orientalis* are enhanced in light. However, Zundelevich et al. (2007) reported, that the measured bioerosion rate in case of sponge *Pione cf. vastifica* was  $2.3 \text{ g m}^{-2} \text{ sponge day}^{-1}$ , showing seasonal but not diurnal variations, suggesting that the zooxanthellae harbouring the sponge have no effect on its boring rate.

Specific behaviour of *Pione lampa*, a bioeroding sponge common in sabellariid worm reef in Florida, with respect to its reproduction is described by Schönberg (2002a,b). This sponge species contained asexual reproductive elements: superficial buds and internal gemmules. Whereas buds are interpreted to function as dispersal elements, gemmules will primarily ensure survival under adverse conditions such as smothering, exposure to air and high temperatures. Bioerosion activity of the sponge increases the chance to free gemmules, as the sponge not only etches into calcareous particles cemented into the matrix produced by the worms, but also into the matrix itself. This ability enables the sponge to utilize the reef as substrate. Investigations on a different type of a burrowing organism found in the *C. lampa* Laubenfels species of sponges (Bermuda) revealed that specific cells are responsible for the removal of calcium carbonate chips allowing penetration of sponges in calcareous stones (Rützler and Rieger, 1975). In higher invertebrate penetrants like polychaetes (*Polydora* species), and molluscs (*Urosalpinx* species), dissolved products may be flushed out of the penetration with seawater by movements of the body or of the boring organs between periods of chemical activity, as well as transported across plasma membranes into the organism in exchange for other ions (Carriker and Smith, 1969). Polychaetes are probably the most frequent and abundant marine metazoans in benthic environments (Martin and Britayev, 1998). Among the polychaetous annelids, which for the most part are free-living, crawling, burrowing and tube-dwelling, the setting-up of close associations with other marine invertebrates is a rather common phenomenon. Four kinds of probable worm-borings are known from the Paleozoic Era (600–225 million years ago) (Cameron, 1969).

The “mud worm”, *Polydora websteri*, is a small polychaete borer which lives in the shells of oysters and other molluscs, and has long been considered a pest of bivalves (Lunz, 1940). Its presence may stimulate the mollusc to secrete extra layers of shell around the worm's burrow. In this manner, *Polydora* causes its host to divert energy to shell deposition, and perhaps leaving its weakened host prey to other enemies and diseases. In terms of the boring

processes, Blake and Evans (1973) summarize three mechanisms in *Polydora*: a chemical mechanism, where special glands secrete acid solutions to dissolve substrates; a mechanical mechanism, where the enlarged modified setae on the 5th setiger abrade the substrate; and a combined chemical and mechanical mechanism. *P. websteri* penetrate all layers of the oyster shell, including prismatic, calcite-ostracum, hypostracum, periostracum, and internal conchiolin layers of visible thickness (Haigler, 1969). Worms induced to settle directly on test substrates at room temperature bored chalky deposits within 24 h, calcite-ostracum and hypostracum within 1 week, and conchiolin layers within a month. The author reported that the ability of adult worms and their larvae to bore hard substrates is determined by a chemical agent. This chemical is not *conchiolinase*, for Iceland spar is composed of pure calcite and lacks the conchiolin matrix which binds calcium carbonate crystals together in most oyster shell layers. The adult and larvae of *P. websteri* did produce acid in seawater agar medium with phenol red indicator, and pieces of Iceland spar introduced into the medium after the worms were removed were etched in a manner indistinguishable from etched areas in artificial blisters (Haigler, 1969).

Another *Polydora* species, *Polydora villosa* is found only in living corals colonies, where the infection rates range from 15% to 100% (Liu and Hsieh, 2000). The fine architecture on the inner surface of the U-sharped passages exhibits characteristics of abrasion made by *P. villosa*. The rough characteristics, such as abrasion pitting and etching seen in the inner surface of the U-sharped passages in *P. villosa* are similar to those found in coral skeletal crystals that have been dissolved by hydrochloric acid, acetic acid, or EDTA (Williams and Margolis, 1974). Therefore Liu and Hsieh (2000) suggested that this polychaeta secretes acids to erode the coral skeleton. During the boring period, *P. villosa* might curve its body, allowing minimum exposure to seawater, thus preventing the acid from being diluted.

Chughtai and Knight-Jones (1988) reported about sabellid polychaetes burrowing into limestones. It was shown that *Pseudopotamilla reniformis* and *Perkinsiana rubra* have irregular winding burrows, which penetrate to a distance of about 5 cm into hard limestone and are probably formed mostly by chemical means. Acid mucopolysaccharides are produced by parapodial glands and by the ventral gland shields, as in other sabellids. By producing tubes of such substances, which readily bind calcium, sabellids are pre-adapted for boring into calcareous substrata.

The oldest mollusc bore holes which was identified by Carriker (1961) are some 400 million years old from the Middle Ordovician, and suggest the antiquity of the origin of the boring mechanism. Recently, Harper (2005) reported that 16% of 248 museum specimens of the large Pliocene terebratulid *Apletosia maxima* show evidence of having been attacked by drilling muricid gastropods. For many years investigators have been studying the mechanisms involved in the penetration of hard substrates by the Mollusca. Most of the work done on the *Bivalvia* concerns the mechanical aspects of penetration, while investigations of the *Gastropoda* have been concerned more recently with the chemical aspects of penetration (reviewed in Smith, 1969). It was reported by the same author about differences in the rate of boring between representatives of *Bivalvia* and *Gastropoda*. This phenomenon could be responsible for the ecological reason of biologically induced demineralization in different groups of Mollusca. Thus, the rate of boring by bivalvia mollusc *Penitella conradi*,  $19 \mu\text{m day}^{-1}$ , is much slower than that found for gastropod *Urosalpinx*,  $400 \mu\text{m day}^{-1}$ . This large difference is not surprising, since the gastropod is boring for food while the bivalve is boring for enlargement of its burrow to accommodate increased body size. Carriker and Smith (1969) noted that the time spent by the

gastropod, *Urosalpinx*, in mechanical abrasion by the radula is much shorter (40–60 s) than the period of chemical dissolution (25–30 min) during each mechanochemical cycle. This difference is even greater in the case of *P. conradi* where chemical dissolution goes on for very long periods (6–8 h) before any mechanical abrasion takes place.

Carriker et al. (1967, 1974), Carriker (1961) and Carriker and Williams (1978) determined that the boring of holes in the shell of bivalve prey by predatory muricid and naticid gastropods, to obtain food, consists of two alternating phases: (i) chemical, in which an accessory boring organ (ABO) or *demineralization gland*, secretes an uncharacterized substance that etches and weakens the shell at the site of penetration, and (ii) mechanical, during which the radula rasps off and swallows some of the weakened shell as minute flakes. However, it is generally believed that chemical boring has evolved as a specialisation of mechanical boring (Morton and Scott, 1988).

Development of a microelectrode has enabled in 1967 the first continuous recording of the pH of the secretion of the normally functioning ABO of the shell-boring predatory snail *Urosalpinx*. The recording was made in an incomplete borehole in a glass-shell model. The minimum pH recorded was 3.8; hitherto the secretion had been considered neutral (Carriker et al., 1967).

The ABO was first described in *Dolium galea* (Naticidae) by Troschel (1854). Schiemenz (1891) first suggested that this ABO secretes an acid. Ankel (1937), by placing freshly cut naticid ABOs against the shell, obtained shallow dissolution in a few hours and postulated the presence of a *calcase*. In 1978 Carriker and Williams hypothesized that a combination of HCl, chelating agents, and enzymes in a hypertonic mucoid secretion released by the ABO dissolve shell during hole boring. The similarity of patterns of dissolution etched by the ABO secretion and those produced artificially by HCl and EDTA as reported by Carriker (1978) support the hypothesis that these chemicals, or chemicals similar to them, are constituents of the ABO secretion. Lactic and succinic acids and a chitinase-like enzyme were also suggested as possible agents in shell dissolution (Carriker and Williams, 1978).

The fine structure of shell etched by the secretion was contrasted in these experiments with normal shell and shell solubilized artificially. A synoptic series of scanning electron micrographs of representative regions of the normal shell of *Mytilus edulis* was prepared to serve as a standard for ultrastructural interpretations of the pattern of dissolution (Carriker, 1978). It was suggested that preferential dissolution of shell matrix by the ABO secretion is functionally advantageous to boring gastropods because it increases the surface area of mineral crystals exposed to solubilization and facilitates removal of shell units from the surface of the borehole by the radula.

Day (as reported in Carriker and Smith, 1969) in a study of the shell-dissolving secretion of the snail, *Agrobuccinum*, found that  $\text{H}_2\text{SO}_4$  is present and accounts for 67% of the  $\text{CaCO}_3$  dissolving activity of the secretion; the remaining solubilization of the shell is achieved by some other unidentified component which may be a chelating agent.

Boring molluscs, rather than rasping organisms, have a significant effect on the mechanical stability of the coral reef framework, since they remove material from the interior. In his impact study, Lazar (1991) measured total alkalinity changes as a direct clue to the rate and mechanism of boring of the bivalve *Lithophaga lessepsiana* in colonies of the coral *Stylophora pistillata*. His experiments included comparison between total alkalinity measurements of seawater surrounding colonies of *S. pistillata* free of *L. lessepsiana* and colonies infected with it. It is suggested that *L. lessepsiana* is able to redissolve chemically up to 40% of the  $\text{CaCO}_3$  deposited by coral.

Another example of biological demineralization is the case of hard tissues of higher mammals. Bone and teeth suffer from mineral loss due to the bacterial activity which results in the development of an acidic environment followed by dissolution (Bryers and Ratner, 2006; Amaechi et al., 1999; Arends and Jongbloed, 1977).

### 3. Enzymes and their role in decalcification

It is generally agreed that enzymes play a role in biomineralization/demineralization/remineralization phenomena. The principal enzymes of those mentioned in the literature are carbonic anhydrase, alkaline phosphatase (Chave, 1984), phosphoprotein phosphatase (Kreitzman et al., 1969; Kreitzman and Fritz, 1970) and vacuolar-type  $\text{H}^+$ -ATPase (Ziegler et al., 2004a,b). Carbonic anhydrase speeds equilibrium reactions in the  $\text{CO}_2$ - $\text{H}_2\text{O}$  system, whereas alkaline phosphatase decouples inorganic phosphorous from organophosphorous compounds. Both enzymes commonly occur at sites of carbonate and phosphate mineralization, and also at many noncalcifying sites and in noncalcifying organisms.

#### 3.1. Carbonic anhydrase (CA)

A related milestone in the evolution of complex life was the evolution of the capacity to catalyze the hydration of  $\text{CO}_2$  (Jackson et al., 2007). The generation of carbon dioxide in processing metabolic wastes and its concomitant equilibration in the aqueous medium:



is important in regulating pH, fixing carbon, and transporting ions across organic membrane (Chave, 1984). The metalloenzyme CA is pivotal to these processes by catalyzing reaction (3) approximately one million fold (Lindskog, 1997). Using a paleogenomic approach, including gene and protein expression techniques and phylogenetic reconstruction, Wörheide and co-workers (Jackson et al., 2007) recently showed that a molecular component of this toolkit was the precursor to the  $\alpha$ -CA, a gene family used by extant animals in a variety of fundamental physiological processes. The authors used coralline demosponge *Astrosclera willeyana*, a “living fossil” that has survived from the Mesozoic, to provide insight into the evolution of the ability to biocalcify, and show that the  $\alpha$ -CA family expanded from a single ancestral gene through several independent gene duplication events in sponges and eumetazoans.

The issue however is: what is the role of carbonic anhydrases in biological decalcification?

The participation of the CA in shifting solubility equilibrium, resulting in the deposition of calcium carbonate by invertebrates, is well established. CA has been implicated in the dissolution of carbonate as well. The enzyme has been found in boring sponges, in the accessory boring organ of the shell-boring muricid gastropods, and its activity has been related to the process of excavating calcium carbonate substrata by acrothoraccian cirripeds and muricid gastropods (reviewed by Hatch, 1980).

Concentration of  $\text{Ca}^{2+}$  in tissues of boring sponge *Cliona celata* is related to the excavating activity of the sponge. It suggests that enzyme, which appears to be associated with mitochondrial-sized particles, is involved in the physiological mechanism of penetration. This conclusion is supported by evidence that CA inhibition results in inhibition of the excavating ability of the sponge. Hatch (1980) proposed several plausible mechanisms for the participation of CA in the penetration of both organic and inorganic components of shell substrate. First, CA, within the filopodial

basket, could accomplish the dissolution of  $\text{CaCO}_3$  by simply providing hydrogen ions for transport across the membrane. Second, in clonid etching cells the exchange of hydrogen for bicarbonate ions would result in both the dissolution of the substratum and a lowering of the pH, with possible optimization for the enzymes responsible for the dissolution of the organic matrix. It is also possible that the  $\text{H}^+$  ions resulting from the activity of CA participate only indirectly in the demineralization of the substratum by proving pH optimization for the activity of chelating agents and/or the enzyme responsible for the breakdown of the organic matrix.

Measurement of CA activity in homogenates of ABO of the muricid gastropod, *Purpura lapillus* showed that enzyme is always present in boring as well as in inactive ABOs, but in variable amounts (Chetal and Fournie, 1969). Experiments *in vivo* on inhibition and activation demonstrated clearly that CA remains intracellularly and is responsible for demineralization of the valves of lamellibranches by *Purpura*. It was shown that action of pure  $\text{CO}_2$  or mixtures of  $\text{CO}_2$  and  $\text{O}_2$  accelerated boring: in the optimal mixture, three times more boreholes were produced by snails than in the controls, and in about half time. Under these conditions the reaction catalyzed by CA goes to the right with hydration of  $\text{CO}_2$ , the reaction is intensified and results in an additional release of  $\text{H}^+$  ions. Consequently, destruction of  $\text{CaCO}_3$  by the ABO of *Purpura* in seawater enriched with  $\text{CO}_2$  is accelerated (Chetal and Fournie, 1969).

It was reported that CA could be also located in different compartments of octocorals (Lucas and Knapp, 1996) and crustaceans (Meyran et al., 1987) to carry out different aspects of the processes of mineralization and demineralization.

### 3.2. Phosphoprotein phosphatase

In 1969 Kreitzman et al. reported that the enzyme phosphoprotein phosphatase can catalyze the rapid demineralization of tooth enamel. This enzyme, which has no apparent proteolytic activity and does not appear to hydrolyze synthetic hydroxyapatite, acts by dephosphorylating the mineralized phosphoprotein matrix of the enamel. Moreover, Kreitzman and Fritz (1970) presented evidence indicating that phosphoprotein phosphatase, which has been implicated in the destruction of enamel and dentin may also be operative in the destruction of bone. This suggests that the enzyme has a role in the resorption of bone mineral that is similar to its role under physiologic and pathologic conditions (Kreitzman et al., 1970). Moreover the release of species from enzymes has been shown to stimulate bone resorption (Gustafson and Lerner, 1984).

### 3.3. Vacuolar-type $\text{H}^+$ -ATPase

Vacuolar-type  $\text{H}^+$ -ATPase plays also a significant role in biological decalcification. Demineralization of the bone matrix requires acidification of this extracellular compartment. Thus, proton extrusion into an extracellular resorption compartment is an essential component of bone degradation by osteoclasts (Nordström et al., 1997). Osteoclasts as the major cellular agents specialized for bone resorption (Inoue et al., 1999) generate a massive acid flux to mobilize bone calcium (Carano et al., 1993). Along bone surfaces, active osteoclasts form the resorptive lacunae, where they can form an enclosed microenvironment composed of highly convoluted membrane infoldings, i.e., “ruffled border”, and a clear zone tightly sealed against the bone surface. Within the enclosed resorption lacuna, osteoclasts secrete acids and various hydrolytic lysosomal enzymes, metalloproteinases, cathepsins, and others for the destruction of inorganic and organic

components of the bone matrix (Inoue et al., 1999). Local extracellular acidification by polarized vacuolar-type  $\text{H}^+$ -ATPase, balanced by contralateral  $\text{HCO}_3^-$ - $\text{Cl}^-$  exchange to maintain physiological intracellular pH, is theorized to drive this process (Carano et al., 1993). This phenomenon is much like the extrusion of protons from the accessory boring organ (ABO) to dissolve molluscan shells and other calcareous substrata.

Clelland and Saleuddin (2000) investigated vacuolar-type ATPase in the ABO of mollusc *Nucella lamellosa* (Gastropoda) with respect to its role in shell demineralization and penetration. The active gap region of the ABO is composed of tall, mitochondria-rich cells with distinct brush borders at their apices, surrounding a hemolymph-containing central sinus. Using electron immunohistochemical methods it was unambiguously shown that a vacuolar-type proton transporting ATPase is present in the brush border of the accessory boring organ of *N. lamellosa*, and is responsible for acidifying secretion from this gland. On the basis of their findings Clelland and Saleuddin proposed model of the mechanism of proton transport in the muricid ABO (Fig. 2).

Recently, Ziegler et al. (2004a,b) investigated expression and polarity reversal of vacuolar-type  $\text{H}^+$ -ATPase during the mineralization–demineralization cycle in terrestrial isopod crustacean *Porcellio scaber* sternal epithelial cells. Isopods molt by shedding first the posterior and then the anterior half of their mineralized cuticle and replace it by a new larger one to allow for growth. About 1 week before the molt, terrestrial species resorb  $\text{Ca}^{2+}$  and  $\text{HCO}_3^-$  from the posterior cuticle and store it between the old cuticle of the first four anterior sternites and the anterior aternal epithelium (ASE) as large  $\text{CaCO}_3$  deposits in the form of amorphous calcium carbonate. Between the posterior and anterior molts the sternal these deposits are entirely resorbed within less than 24 h and used for the rapid mineralization of the new posterior cuticle to regain full support and protection. Resorption of the deposits requires the transport of protons across the ASE to mobilize  $\text{Ca}^{2+}$  and  $\text{HCO}_3^-$  ions, which are then transported into the hemolymph. During  $\text{CaCO}_3$  deposit formation and resorption the ASE is differentiated for ion transport. These differentiations include an increased expression of the plasma membrane  $\text{Ca}^{2+}$ -ATPase and of the  $\text{Na}^+/\text{Ca}^{2+}$ -exchanger, increased volume density of plasma membrane proteins, and an increased surface area of the basolateral plasma membrane by a system of ramifying invaginations (Ziegler et al., 2004a,b). Results obtained in these experiments indicate a contribution of a vacuolar-type  $\text{H}^+$ -ATPase to  $\text{CaCO}_3$  deposition and a reversal of its polarity from the basolateral to the apical plasma membrane compartment within the same cells. Thus, similarities between the ABO, osteoclasts, the mantle of freshwater bivalves (Clelland and Saleuddin, 2000) and sternal epithelial cells of crustaceans additionally suggest that the mechanism for decalcification of calcareous substrates *in vivo* is conserved in nature.

## 4. Mechanisms and kinetics of the demineralization of Ca-containing biomaterials

### 4.1. Calcium phosphates

Calcium phosphates are the most significant inorganic constituents of the hard tissues of higher vertebrates. Despite the fact that the main inorganic salt encountered in the calcium phosphates of the biominerals is hydroxyapatite ( $\text{Ca}_5(\text{PO}_4)_3\text{OH}$ , HAP), thermodynamically less stable calcium phosphates including octacalcium phosphate ( $\text{Ca}_8\text{H}_2(\text{PO}_4)_6 \cdot 5\text{H}_2\text{O}$ , OCP) and even dicalcium phosphate dihydrate ( $\text{CaHPO}_4 \cdot 2\text{H}_2\text{O}$ , DCPD) have been reported to be present (Nancollas and Bareham, 1975; Tomazic et al., 1994; Nancollas, 1992). HAP present in biominerals is not

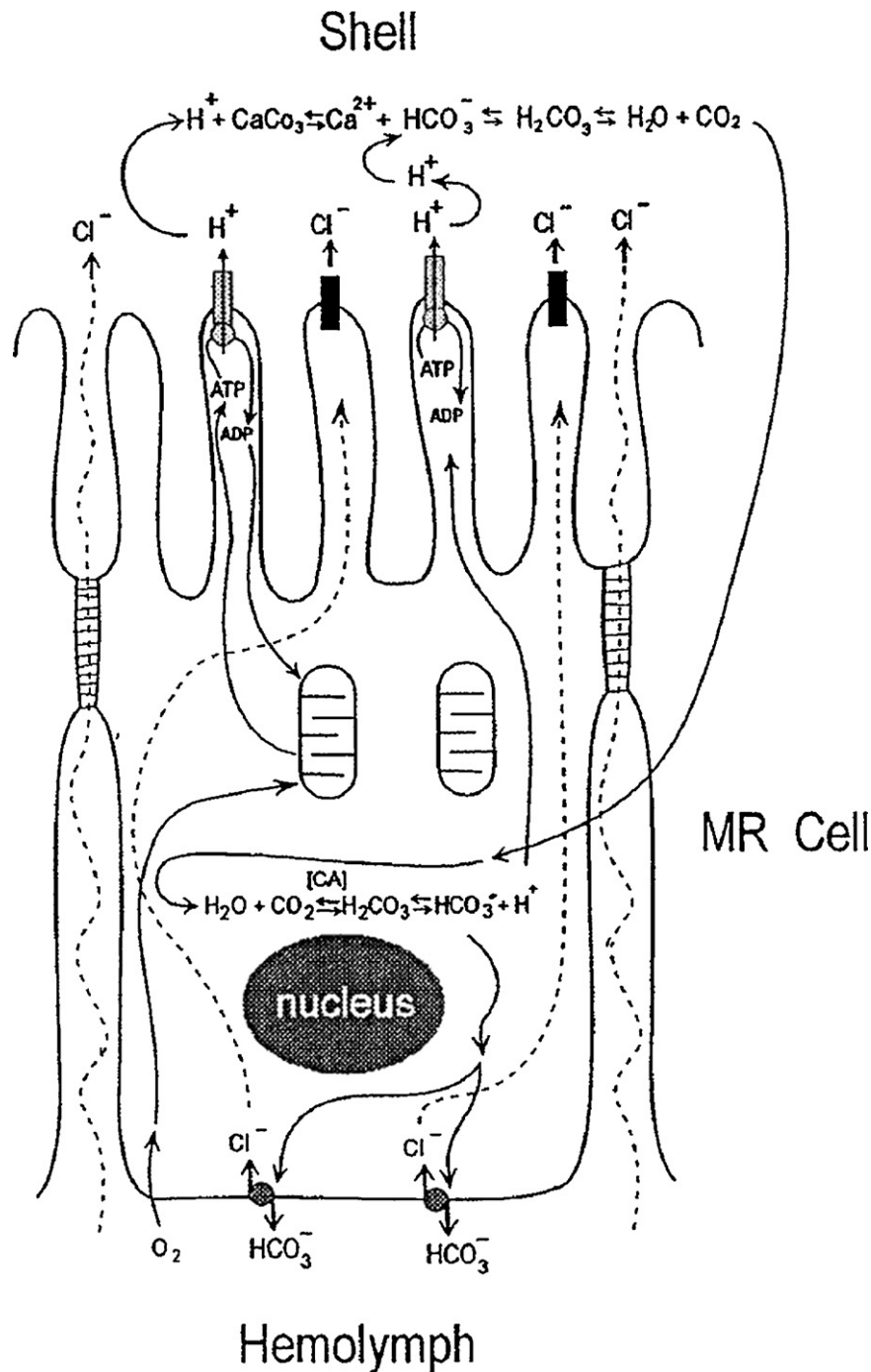


**Fig. 2.** Revised model of the mechanism of proton transport in the muricid accessory boring organ (ABO). Carbonic anhydrase (CA) catalyzes the production of  $\text{H}^+$  and  $\text{HCO}_3^-$  via the carbonic acid pathway. Bicarbonate is removed from the mitochondria-rich (MR) epithelial cell via basal  $\text{HCO}_3^-/\text{Cl}^-$  antiporters, while protons are extruded from the cell into the bore hole by V-ATPase pumps located in the microvilli. Mitochondria generate ATP to power the extrusion process, generate metabolic  $\text{CO}_2$  for the carbonic acid reaction, and provide a reducing environment to stabilize the V-ATPase molecules. Chloride ions exit the cell via apical ion channels, and possibly by paracellular routes. The protons and chloride ions (HCl) act to dissolve the mineralized component ( $\text{CaCO}_3$ ) of the shell, while degradative enzymes also present in the secretions of the ABO break down the organic matrix. Carbon dioxide liberated from the dissolving shell may diffuse into the cell to enhance the carbonic acid reaction. The presence of  $\text{HCO}_3^-/\text{Cl}^-$  antiporters and, as speculated here, of chloride ion channels is based on comparable studies of mitochondria-rich cells in other animal epithelia.

stoichiometric as it is able to incorporate various ions which do not essentially change its structure (Kibby and Hall, 1972). It has been reported that sodium, potassium and magnesium ions exchange for calcium fluoride and chloride for the hydroxyls and carbonate for the phosphate (Trautz, 1967; Weatherell and Robinson, 1973; Young, 1975; Koutsoukos, 1998). Also, the presence also of non-stoichiometric HAP has been documented and a formula corre-

sponding to the compound:  $\text{Ca}_{10-x}(\text{PO}_4)_{6-x}(\text{HPO}_4)_x(\text{OH})_{2-x}\cdot x\text{H}_2\text{O}$  with  $x \leq 2$  has been proposed (Ten Cate, 1979). The deviation of the molar Ca/P ratio found in biological apatites from the value of 1.67 corresponding to the stoichiometric HAP has been ascribed to the presence of  $\text{HPO}_4^{2-}$  ions on the surface or to the cationic substitution into the apatitic lattice (Jenkins, 1978). The solubility of the various calcium phosphates is quite different and depends

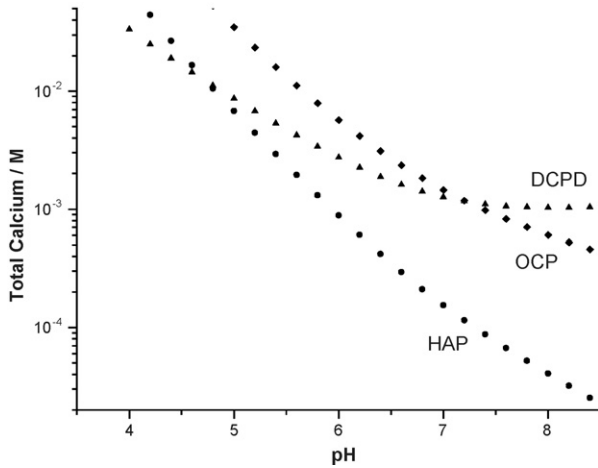


Fig. 3. Solubility isotherms of calcium phosphates calculated for 37 °C, 0.15 M NaCl.

strongly on the solution pH. Solubility isotherms calculated for calcium phosphates which demonstrate the strong pH dependence are shown in Fig. 3.

The de-calcification process of biominerals may be considered as a dissolution process taking place at conditions in which the calcium phosphate phases are undersaturated with respect to the respective fluid with which they are in contact. Interestingly, it has been reported that the dissolution of calcium phosphate phases depends on the preparation method (Dehbi and Thomas, 1987). This observation may have important implications for the dissolution of biominerals, which may form at different sites and under different conditions (physiological or pathological). It is also interesting to note that the dissolution of biological apatites has been shown to differ from the respective process in synthetic materials (Daculsi et al., 1989). More specifically, biological apatite crystallites dissolve from their core as contrasted to the non-specific dissolution of the synthetic crystals. The difference was ascribed to the protein–calcium phosphate interaction. In general, biominerals formation is the result of interactions between mineral growth and biological organization. Bone and teeth are composite-like tissues in which the organic matrix forms a continuum into which the mineral crystallites are dispersed (Veis and Sabsay, 1983). Decalcification, should therefore be envisioned as the interaction of a composite material with an undersaturated fluid environment which is developed among others through the function of cellular material or hormones activity of the various tissues mineralized (Tauchmanova et al., 2006).

#### 4.2. Mechanism and kinetics of the dissolution of Ca-containing biomaterials

From the thermodynamics point of view, a biomineral dissolves in contact with a solution undersaturated with respect to the specific salt. Undersaturation in the microenvironment of the biominerals is developed primarily by pH changes. Quantitatively, undersaturation may be expressed in several types of units (Mullin, 1993a,b). For sparingly soluble salts  $M_{\nu_+}A_{\nu_-}$  the undersaturation ratio is defined as

$$S = \frac{(\alpha_{M^{m+}})_s^{\nu_+} (\alpha_{A^{a-}})_s^{\nu_-}}{(\alpha_{M^{m+}})_\infty^{\nu_+} (\alpha_{A^{a-}})_\infty^{\nu_-}} = \left( \frac{IP}{K_s^0} \right)^{1/\nu} \quad (4)$$

where subscripts s and  $\infty$  refer to solution and equilibrium conditions, respectively,  $\alpha$  the activities of the respective ions and

$\nu_+ + \nu_- = \nu$ . IP and  $K_s^0$  are the ion products in the undersaturated solution and at equilibrium, respectively.

The fundamental driving force for the formation of a salt from a supersaturated solution is the difference in chemical potential of the solute in the undersaturated solution from the respective value at equilibrium:

$$\Delta\mu = \mu_\infty - \mu_s \quad (5)$$

Since the chemical potential is expressed in terms of the standard potential and the activity,  $\alpha$ , of the solute:

$$\mu = \mu^0 + R_g T \ln \alpha \quad (6)$$

Substitution of Eq. (6) to Eq. (5) gives for the driving force for the mineral dissolution:

$$\frac{\Delta\mu}{R_g T} = -\ln \left( \frac{\alpha_s}{\alpha_\infty} \right) = -\ln S \quad (7)$$

For electrolyte solutions the mean ionic activity is taken:

$$\alpha = \alpha_\pm^{\nu} \quad (\nu = \nu_+ + \nu_-) \quad (8)$$

and

$$\frac{\Delta\mu}{R_g T} = -\ln \left( \frac{\alpha_{\pm,s}}{\alpha_{\pm,\infty}} \right)^{1/\nu} = -\frac{1}{\nu} \ln S \quad (9)$$

The rates of dissolution may be defined as the velocity of recession of a crystal face relative to a fixed point of the crystal. This definition however cannot be easily applied to the formation of polycrystalline deposits such as those encountered in the biomineral composites. In this case, experimentally the rates of dissolution may be expressed by equation:

$$R_d = \frac{(dm/dt)}{A} \quad (10)$$

where  $m$  is the number of moles of the mineral in contact with the undersaturated solution and  $A$  is the surface area of the substrate (Wang et al., 2006a,b,c).

#### 4.3. Models for the dissolution process

The models developed to describe quantitatively crystal growth and dissolution have followed two major approaches: diffusion-reaction and surface layer dissolution. A thorough review on the dissolution mechanisms involved in the dissolution of calcium phosphates has been presented by Dorozhkin (2002).

##### 4.3.1. Diffusion-reaction theory

According to the Noyes–Whitney theory crystals may be considered to dissolve by the building units and their subsequent transfer into the bulk solution. The rate of disintegration of the crystals by this growth unit removal depends on the concentration difference between the crystal surface and the bulk solution. The process of dissolution takes place in two stages: (i) detachment of the crystal building units from the crystal network and (ii) transfer of the units to the bulk solution by diffusion. Step (i) is thus a reaction step and step (ii) is diffusion. The mathematical description of the two steps is respectively:

$$\begin{aligned} \left. \frac{dc}{dt} \right|_R &= k_R (c_\infty - c_s) \quad (\text{reaction}) \\ \left. \frac{dc}{dt} \right|_D &= k_D (c_s - c_b) \quad (\text{diffusion}) \end{aligned} \quad (11)$$

where  $(dc/dt)|_R$ ,  $(dc/dt)|_D$  are the rates corresponding to reaction and diffusion, respectively,  $k_R$  and  $k_D$  the respective rate constants and  $c$  is the solute concentrations. The subscripts  $\infty$ , s and b refer to

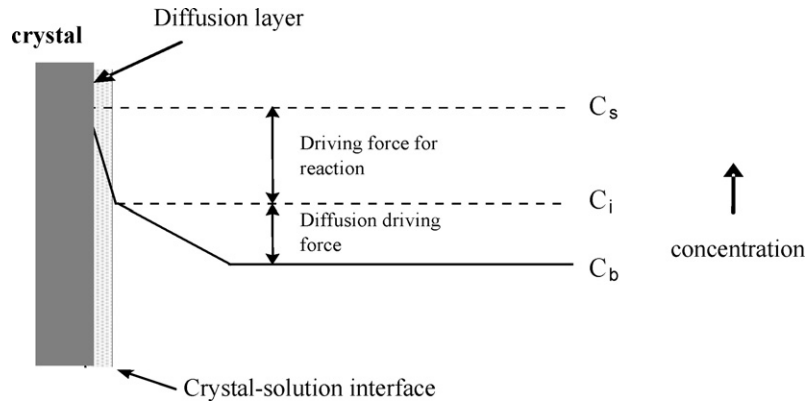


Fig. 4. The dissolution process according to the reaction-diffusion theory.

equilibrium, surface and bulk, respectively, and  $n$  is the reaction order. The rate constants  $k_R$ ,  $k_D$  cannot be experimentally measured in a polycrystalline system as they are different for different crystal faces. The prevalence of reaction or diffusion depends on the relative magnitudes of  $k_R$  and  $k_D$ . The two steps are schematically shown in Fig. 4. When steady state conditions are established the two rates are equal and the slowest step determines the prevalent mechanism (Sjöberg and Rickard, 1983).

The value of the reaction order has in several cases been determined from experimental results that it is  $n = 1$ . Since the dissolution rate constant is

$$k_D = \frac{D}{\delta} \quad (12)$$

where  $D$  is the molar diffusion coefficient and  $\delta$  is the diffusion layer thickness at the steady-state, Eq. (11) yield:

$$k_g(c_\infty - c_s) = k_D(c_\infty - c_b) \quad (13)$$

from which

$$c_\infty = \frac{k_R c_\infty + k_D c_b}{k_R + k_D} \quad (14)$$

Substitution of Eq. (14) into one of Eq. (11) yields:

$$\text{Rate} \equiv R = \frac{dc}{dt} = k_0(c_\infty - c_b) \quad (15)$$

where

$$k_0 = \frac{k_g K_P}{k_R + k_D} \quad (16)$$

Eq. (15) is a mathematical expression correlating the rates of dissolution measured experimentally (e.g. from calcium increase in undersaturated solutions as a function of time) with the solution undersaturation which is the deviation of the solute concentration in the solution from equilibrium. Eq. (15) for salts of electrolytes, the quantity for the analytical concentration,  $c$  should be replaced by mean ion activities. A typical value for  $D$ , the molar diffusion is  $10^{-9} \text{ m}^2 \text{ s}^{-1}$ . The diffusion layer thickness may be calculated according to (Mullin, 1993a,b):

$$\delta = \frac{3L}{2} \left( \frac{\rho_s u L}{\eta} \right)^{1/2} \left( \frac{\eta}{\rho_s D} \right)^{-1/3} \quad (17)$$

where  $L$  is the diameter of the dissolving crystallites in a polycrystalline system,  $\rho_s$  the density of the aqueous solution in which dissolution takes place ( $10^3 \text{ kg/m}^3$ ),  $u$  the linear velocity of the dissolving particles and  $\eta$  is the viscosity of the undersaturated

aqueous solution ( $0.8904 \times 10^{-3} \text{ kg } 5^{-1} \text{ m}^{-1}$  at  $25^\circ\text{C}$ ). It is thus possible for an experiment to calculate the diffusion rate constant from Eqs. (12) and (17).

#### 4.3.2. Surface-reaction controlled morphology-based theories

All crystals contain imperfections which includes steps, kinks, terraces, ledges and holes or vacancies. The schematic depiction of a crystal surface is shown in Fig. 5. This model is known as the ‘‘Kossel model’’ (Kossel, 1934). The dissolution proceeds by the detachment of the crystal units in the following steps:

- (i) Detachment from an active site (e.g. kink);
- (ii) Partial hydration of the detached unit;
- (iii) Hydration of the vacant site;
- (iv) Diffusion of the (partially) hydrated unit along the edge of a step;
- (v) Diffusion of the unit along the step and completion of hydration;
- (vi) The unit is transferred to the bulk solution through the diffusion boundary layer on the crystal surface.

The slowest of the steps (i)–(vi) is the rate-determining step. Since hydration reactions are in general very fast, the mechanism is determined either by step (iv) or (vi). In case diffusion to the bulk solution is the rate determining step the treatment is similar to that described before for diffusion. The surface diffusion may be described by three different models shown schematically in Fig. 6. As may be seen in Fig. 6A it is possible to start dissolution from one center from which originates the units detachment leading to step disintegration.

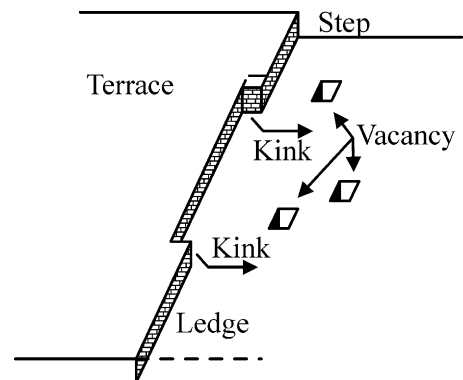


Fig. 5. Surface of a crystal according to Kossel. The various types of dislocations are shown.

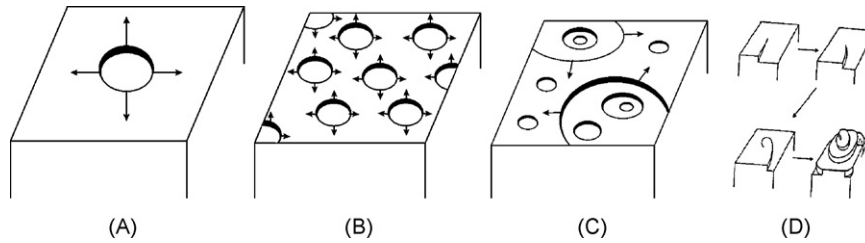


Fig. 6. (A) Mononuclear model. (B) Polynuclear in one crystal step. (C) Polynuclear in multiple steps: birth and spread. (D) Spiral model.

It is also possible that detachment takes place simultaneously from multiple centers (Fig. 6B and C) which may be developed in one or more, steps on the crystal surface. Alternatively, it has been suggested that the crystal units' detachment takes place along spirals originating from an active site on the crystal surface following an Archimedian spiral (Fig. 6D). The unit detachment along the spirals takes place at constant velocity. The dissolution mechanisms presented describe quantitatively the dissolution by equations relating the experimentally measured rates of dissolution as a function of the solution undersaturation which is the necessary condition for dissolution. The rate expressions for the various models are as follows:

For the mononuclear model (Fig. 6A):

$$R = A \exp\left(\frac{-\pi h \gamma^2 \nu}{k^2 T^2} \ln S\right) \quad (18)$$

where  $A$  a constant including the total crystal surface area available,  $h$  a crystal step height,  $\gamma$  the surface energy,  $\nu$  the molecular volume of the dissolving crystal,  $k$  the Boltzmann constant,  $T$  the absolute temperature and  $S$  is the solution undersaturation.

According to the polynuclear model (Fig. 6B and C). The rate expression is

$$R = A \left(\frac{\gamma \nu}{kT}\right)^2 (\ln S)^{-3/2} \exp\left(\frac{-B}{T^2} \ln S\right) \quad (19)$$

where  $B$  is a constant. A similar expression was given by Zhang and Nancollas (1991):

$$R = k_d \sigma^{2/3} (-\ln S)^{1/6} \exp(-A/\ln S) \quad (20)$$

where  $A$  is a constant:

$$A = \left(\frac{\pi}{3}\right) \left(\frac{\gamma}{kT}\right)^2 \quad (21)$$

Transformation of Eq. (20) in a linear form yields:

$$\ln \frac{R}{\sigma^{2/3} (-\ln S)^{1/6}} = \ln k_d - \frac{A}{\ln S} \quad (22)$$

For the spiral dissolution model the dependence of the rates on the solution undersaturation is

$$R = C \frac{\sigma^2}{\sigma_1} \tanh \frac{\sigma_1}{\sigma} \quad (23)$$

where  $C$  and  $\sigma_1$  are constants involving step size and crystal unit jump frequencies related with their migration along the spirals. For low undersaturation values (close to equilibrium) Eq. (23) is reduced to:

$$R = C \frac{\sigma^2}{\sigma_1} \quad (24)$$

which predicts a parabolic dependence of the rates of dissolution on the solution undersaturation. For large deviations from

equilibrium ( $\sigma \gg \sigma_1$ ) Eq. (23) yields:

$$R = C \sigma \quad (25)$$

As may be seen therefore it is possible to deduce the mechanism of dissolution of crystals according to the above-described models, depending on the fit of the rates measured on the solution undersaturation. It should however be kept in mind that it is possible that more than one mechanisms are operative, depending on the solution undersaturation.

The possibility of a calcium phosphate biomineral to dissolve depends on the value of the Gibbs free energy change for the transition undersaturated  $\rightarrow$  saturated solution. For the biologically important minerals, HAP, OCP and DCPD the expressions for this free energy change, which is the respective thermodynamic drive force are as follows:

For DCPD:

$$\Delta G_{\text{DCPD}} = \frac{RT}{2} \ln \frac{(\text{Ca}^{2+})(\text{HPO}_4^{2-})}{K_{s,\text{DCPD}}^0} \quad (26)$$

for OCP

$$\Delta G_{\text{OCP}} = \frac{RT}{16} \ln \frac{(\text{Ca}^{2+})^8 (\text{H}^+)^2 (\text{PO}_4^{3-})^6}{K_{s,\text{OCP}}^0} \quad (27)$$

and for HAP

$$\Delta G_{\text{HAP}} = \frac{RT}{9} \ln \frac{(\text{Ca}^{2+})^5 (\text{PO}_4^{3-})^3 (\text{OH}^-)}{K_{s,\text{HAP}}^0} \quad (28)$$

In the logarithmic term, the ratio of the ionic product to the respective thermodynamic solubility product is the saturation ratio,  $S$ . For undersaturated solutions in all cases  $S < 1$  and therefore the respective. Change in the thermodynamic driving force is  $< 0$ , i.e. dissolution takes place upon contact of the crystals with the undersaturated solutions. In the kinetics studies, it is often the relative undersaturation,  $\sigma$ , which is used defined as

$$\sigma = S - 1 \quad (29)$$

In Eqs. (26)–(28) the quantities in parentheses are the activities of the respective ions. The thermodynamic solubility products for the biominerals considered are:  $2.32 \times 10^{-7} \text{ M}^2$  for DCPD (Tang et al., 2001),  $2.51 \times 10^{-99} \text{ M}^{16}$  for OCP (Shyu et al., 1983) and  $5.52 \times 10^{-118} \text{ M}^{18}$  for HAP (McDowell et al., 1977). The computation of the activities of free ions in complex solutions requires taking into account all equilibria involved, together with the mass and charge balance equations. Moreover, suitable expressions for the ion activity coefficients are needed. Activity coefficients may be expressed as a function of the solution ionic strength,  $I$ , using various semi-empirical equations. Davies equation:

$$\log f_z = -Az^2 \left( \frac{\sqrt{I}}{1 + \sqrt{I}} - 0.3I \right) \quad (30)$$

has been suggested as a reasonably good expression for the ionic strength of 0.15 M, typical for most of the biological fluids (Nancollas, 1966).

The kinetic expression often used to describe dissolution of sparingly soluble salts is a first order relationship between the rate of dissolution,  $R$  and the solution undersaturation:

$$R = k_{\text{diss}}(C_e - C_u) \quad (31)$$

where  $k_{\text{diss}}$  is the rate constant and  $C_e$ ,  $C_u$  are the concentrations of the solute at equilibrium and in the undersaturated solution, respectively. Eq. (28) is not always valid (Patel et al., 1987; Gramain et al., 1989; Christoffersen and Christoffersen, 1992; Melikhov et al., 1990).

In general the overall dissolution process is interpreted by a power law of the type:

$$R = k_{\text{diss}}\sigma^n \quad (32)$$

where  $n$  is a power indicative of the mechanism. For HAP dissolution in the pH range between 5.0 and 7.2 the rates were found to be slower by four orders of magnitude with respect to the rates corresponding to diffusion according to Fick's law (Nancollas, 1989). Concerning the mechanism of dissolution of calcium phosphates it seems that there is no consensus. For HAP, e.g., the thermodynamically most stable phase, both surface diffusion (Christoffersen and Christoffersen, 1979; Margolis and Moreno, 1992; Valsami-Jones et al., 1998) and mass transport controlled mechanisms (Brown and Chow, 1981; Lower et al., 1998), have been proposed. Considerable help in understanding mechanisms in dispute is the development of modern experimental techniques (e.g. the potentiometric techniques combined with SEM (Brown and Chow, 1981; Lower et al., 1998) and AFM (Valsami-Jones et al., 1998; Wang et al., 2006a,b,c; Koutsoukos and Valsami-Jones, 2003) for the investigation of the kinetics of these processes. DCPD dissolution was found to be controlled by surface diffusion and the dissolution data fitted to a spiral dissolution mechanism (Nancollas, 1989). A significant advance in understanding the mechanism of dissolution came with the development of a methodology to perform dissolution studies at constant saturation (Budz and Nancollas, 1988; Tang and Nancollas, 2002; Tang et al., 2001; Chow et al., 2003; Paschalis et al., 1996). The methodology was applied to tooth enamel studies (Chen and Nancollas, 1986.) and it was concluded that the mechanism of dissolution was surface diffusion controlled. Further studies on tooth demineralization at conditions of constant undersaturation led to the conclusion that the rates of dissolution are higher inside the lesions in comparison with the respective values on the surface of the tooth enamel (de Rooij and Nancollas, 1984). A modification of the constant composition methodology, using two different probes to monitor the dissolution process was also successfully applied for mixed calcium phosphate phases (Tang et al., 2003). Maintenance of constant undersaturation during the course of dissolution provides information for the dissolving biominerals at pseudo steady state conditions, mimicking physiological conditions. It is particularly informative for monitoring dissolution at the initial stages. It is at this critical point that methods relying on variable saturation fail, because of the fast changes in the solution saturation with respect to the mineral phase investigated. At constant undersaturation not only the rates of dissolution can be precisely measured thus obtaining reliable mechanistic information (through rate-undersaturation correlation) but also the effect of the presence of impurities and/or additives may be investigated. It was thus found that the rates of dissolution of biological apatites containing ionic impurities decreased as a function of time despite the fact that undersaturation, the driving force for dissolution, was kept

constant (Nancollas, 1989; Chen and Nancollas, 1986.). The dissolution of carbonated apatites, considered as models for biominerals has revealed that carbonate was preferentially released (Mayer et al., 1988; Budz et al., 1988a,b). In most cases however, it may be concluded that the mechanism of dissolution of biominerals is surface diffusion controlled. The rates therefore of demineralization of biological phosphate salts are controlled by the surface, which means that interactions at the surface either with macromolecules or with ions should be carefully considered in the design of experiments *in vitro*. Eight different dissolution models of calcium apatites (both fluorapatite and hydroxyapatite) were also analyzed in review by Dorozhkin (2002).

#### 4.3.3. Phenomenological surface coordination models: case studies of effect of organic ligands on calcium and magnesium carbonates dissolution

Carbonate mineral dissolution kinetics has been an issue of active research efforts in relation to biomineralization (Boquet et al., 1973; Morita, 1980; Monger et al., 1991; Pokrovsky and Savenko, 1994, 1995; Ferris et al., 1994; Fujita et al., 2000; Warren et al., 2001; Ferris et al., 2003; Dittrich and Obst, 2004; Lian et al., 2006; Mitchell and Ferris, 2006; Rodriguez-Navarro et al., 2007). Numerous laboratory experiments demonstrated that the dissolution of carbonates (calcite and magnesite) is controlled by pH, concentration of  $\text{HCO}_3^-/\text{CO}_3^{2-}$  ions, and temperature. Despite a number of studies on calcite dissolution in the presence of organic ligands (Perry et al., 2004, 2005; Fredd and Fogler, 1998a,b; Wu and Grant, 2002; Frye and Thomas, 1993; Hoch et al., 2000; Thomas et al., 1993; Compton and Sanders, 1993; Compton and Brown, 1995; Spanos et al., 2006a,b), rarely the effect of variable ligand concentration on the dissolution rate has been rigorously quantified. There are a few data on magnesite dissolution in the presence of ligands at some technologically relevant solution conditions (Hamdona et al., 1995; Demir et al., 2003; Laçin et al., 2005; Bayrak et al., 2006) and Jordan et al. (2007) studied ligand-controlled magnesite dissolution at 100 °C and low  $\text{pCO}_2$  in the presence of a single concentration (0.01 M) of organic and inorganic ligands via a combination of macroscopic rate measurements and hydrothermal AFM. In order to extend the range of ligand concentrations to broader environmental conditions, Pokrovsky et al. (2008) performed detailed study on calcite and magnesite dissolution in the presence of variable ( $10^{-5}$  to  $10^{-2}$  M) ligand concentrations at conditions pertinent to  $\text{CO}_2$  storage basins (60 °C, 30 atm  $\text{pCO}_2$ , pH 4.5–5.5). Recently, Golubev et al. (submitted) studied calcite dissolution in the presence of 16 organic ligands ranging in the concentration from  $10^{-6}$  M to 0.03 M at otherwise constant solution parameters (25 °C, 0.1 M NaCl, pH 8.5). These organic ligands represent simple low-molecular weight organic acids (carboxylates, chelates, and aromatic compounds) and analogs of bacterial exometabolites, external cell envelopes, and natural polymers (humic acids). The following order of ligand effect on calcite dissolution at 0.03 M ligand concentration has been established: Gum xanthan < gluconate < alginate < fumarate  $\cong$  NaCl < malonate  $\sim$  succinate  $\leq$  acetate < L-glutamate < 2,4-dihydroxybenzoate (DHBA)  $\sim$  glucosamine  $\sim$  phthalate  $\sim$  gallate  $\leq$  pectin < 3,4-DHBA  $\ll$  citrate  $\ll$  EDTA (Fig. 7).

The effect of organic ligands on calcium carbonate dissolution can be rationalized within the framework of the surface coordination approach assuming the overall dissolution rate is controlled by reactions promoted at Ca centers by various ligands which compete for available surface sites (Stumm, 1992). The effectiveness of ligands depends on the molecular structure and thermodynamic stability of the surface complexes they form. For example, especially efficient are ligands whose functional groups

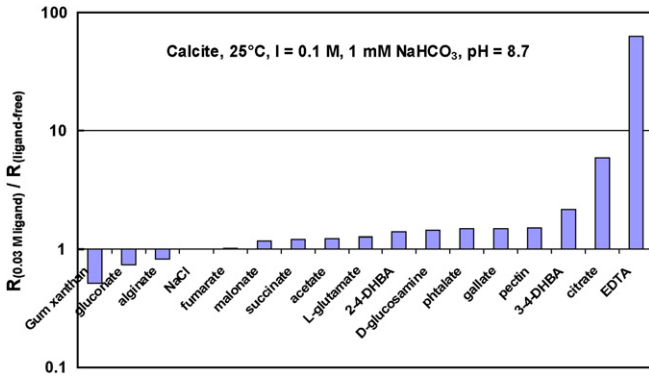
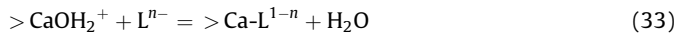


Fig. 7. The ratio of calcite dissolution rate in the presence of 0.03 M ligand to that in the absence of ligand. Gum xanthan, gluconate, and alginate act as inhibitors of calcite dissolution and citrate and EDTA are the strongest enhancers of dissolution (Golubev et al., submitted).

contain two or more oxygen donors and which can form bi- or multidentate mononuclear surface chelates (Stumm, 1992). In contrast, ligands forming bi- or polynuclear complexes, that can bridge two or more metal centers at the surface lattice, are known to retard dissolution.

In order to quantitatively model the effect of ligand on carbonate dissolution rate, the simplest, bimolecular surface reaction between positively charged surface groups ( $>\text{CaOH}_2^+$ ) and negatively charged ligands ( $\text{L}^{n-}$ ) can be considered:



According to this scheme, the rate of ligand-controlled dissolution is proportional to the concentration of the surface center–ligand complex  $>\text{Ca-L}^{1-n}$  which can be deduced from the reaction (3) stability constant ( $K_{\text{Ca-L}}^*$ ):

$$K_{\text{Me-L}}^* = \frac{\{>\text{Ca-L}^{1-n}\}}{\{>\text{CaOH}_2^+\} \times [\text{L}^{n-}]} \quad (34)$$

It is reasonable to assume that, in the presence of a ligand, the calcite forward dissolution rate is thus the sum of  $\text{H}_2\text{O}$ –( $R_{\text{H}_2\text{O}}$ ) and ligand-controlled dissolution, similar to that of brucite (Pokrovsky et al., 2005), dolomite (Pokrovsky and Schott, 2001), smectite (Golubev et al., 2006), and diopside (Golubev and Pokrovsky, 2006):

$$R = k_{>\text{CaOH}_2^+} \times \{>\text{CaOH}_2^+\} + k_{>\text{Ca-L}} \times \{>\text{Ca-L}^{1-n}\} \quad (35)$$

In Eq. (35),  $k_{>\text{CaOH}_2^+}$  is the rate constant for water-promoted dissolution reaction measured in the absence of ligand at given pH and  $p\text{CO}_2$  and  $k_{>\text{Ca-L}}$  is the empirical kinetic constant pertinent to each ligand. The simplified phenomenological equation for calcite and magnesite dissolution in the presence of ligands can be obtained by combining Eqs. (34) and (35):

$$R = k_{>\text{CaOH}_2^+} \left( 1 - \frac{K_{\text{Ca-L}}^* [\text{L}^{n-}]}{1 + K_{\text{Ca-L}}^* [\text{L}^{n-}]} \right) + k_{>\text{Ca-L}} \frac{K_{\text{Ca-L}}^* [\text{L}^{n-}]}{1 + K_{\text{Ca-L}}^* [\text{L}^{n-}]} \quad (36)$$

Note that the stability constants for surface adsorption reactions ( $K_{\text{Ca-L}}^*$ ) correlate with corresponding values for association reactions in homogeneous aqueous solution as it is the case for other simple oxides (Schindler and Stumm, 1987; Ludwig et al., 1995; Pokrovsky et al., 2005).

## 5. Demineralization of naturally occurring Ca-containing biocomposites

### 5.1. Bone

Bone is a hierarchically structured composite material in the engineering sense and its properties may differ significantly from those of the individual components. The function of the composite material depends not only on the chemistry of the components but also on their relative orientation in the structure. Modern views on the bone structure and formation including such aspects as transient precursor strategy in mineral formation of bone (Crane et al., 2006; Weiner, 2006; Grynpas and Omelon, 2007), mechanisms of intrafibrillar (Olszta et al., 2007) and self-assembly (Cui et al., 2007) mineralization of collagen as main organic template are recently actively discussed.

Reports on bone demineralization date back to 1889 upon exploration of using demineralized bone for surgical implantation (Senn, 1889). This approach was successful in rats and resulted in ligament reconstruction (Yamada, 2004). The history of bone demineralization is represented in detail in the first part of our review (Ehrlich et al., 2008). The major problems in obtaining the organic matrix of bone is, first, that very few of the proteins or the complex proteoglycans can be extracted without first solubilizing the calcium-phosphate (Ca-P) crystals. Secondly, the major structural protein of the bone is collagen. While one can solubilize the Ca-P crystals relatively easily (dilute strong acids, EDTA, weak acids such as acetic and citric acids), the fibrous collagen is insoluble after decalcification, especially in its undenatured state (Glimcher et al., 1965). A reasonable number of the very many non-collagenous proteins, such as the phosphoproteins (Gotoh et al., 1990, 1995) including bone sialoprotein (Wang et al., 2006a,b,c) can be solubilized during the decalcification of the bone by a variety of solvents and to varying extents, depending on which solvent is used. Thus, it was reported (Gerstenfeld et al., 1994) that chelation of calcium ions by EDTA and dissolution of the mineral phase by acid extraction released 95% or more of the total calcium content of the bone powder by 48 h, guanidine-HCl released less than 20% or less of the total calcium content even when extraction was carried out by 168 h. Moreover, although guanidine-HCl solubilized a significant amount of collagen as gelatin, essentially none of phosphoproteins, osteocalcin, or the proteoglycan decorin were solubilized, as detected by immunological techniques. In contrast, extraction of the mineralized bone powder by HCl and formic acid was very efficient in selectively solubilizing osteocalcin and osteopontin, while bone sialoprotein was selectively released by EDTA, and solubilized to a lesser extent by formic acid. Similarly, EDTA selectively removed decorin compared with HCl, formic, acetic, or citric acids. These data provide some insight into the intrinsic solubility characteristics of collagen, the specific non-collagenous proteins, and their potential association with each other and the mineral phase.

The distinct differences in the patterns of attack on bone by weakly ionized acids and their buffers as opposed to EDTA helped to define some characteristics of “good” demineralizing agents. Weakly dissociated acids and their buffers produced a rapidly penetrating diffuse attack on mineral of bone (Eggert and Germain, 1979). In contrast, EDTA generated a well-defined front of demineralization. This was a pattern also observed with the strongly ionized trichloroacetic acid. With these latter agents a barrier appears to be established at the front of demineralization that prevents diffusion of calcium salts from the core of the specimen. Such a barrier is not established by acidic buffers with the result that demineralization is more generalized at an early stage. Rapid demineralizing buffers were those producing minimal

secondary reprecipitation of nodules of calcium salts that were rapidly redissolved. Potassium formate and lactate-containing buffers possessed this property and were described therefore as the most rapid agents (Eggert and Germain, 1979). From a kinetic point of view, acid demineralization of the bone specimens consists of the following processes (according to Birkedal-Hansen, 1974): (a) diffusion of acid in the bath toward the specimen surface; (b) diffusion of acid in the organic matrix of the decalcified part of the specimen toward the decalcification front; (c) reaction with hydroxyapatite at the decalcification front; and (d) outward diffusion of reaction products. The exact kinetic treatment of this series of events is complicated and elaborate.

In an attempt to reduce the commonly encountered artifacts of tissue shrinkage obtained with rapid decalcification with strong mineral acids many laboratories have utilized the much slower decalcification achieved with EDTA. This is a gentle, non-acid decalcifying reagent which has the advantage of not damaging the tissue but is slow acting. EDTA demineralization is generally considered to be practically applicable only to small fragments of bone (Belanger et al., 1965).

Demineralization of biological materials has generally been conducted in aqueous media as reported above, resulting in considerable loss of water-soluble material, gross disruption of macromolecular organization and chemical breakdown of many components of biological tissues (Scott and Kyffin, 1978). By working in organic solvents, loss of water-soluble materials should be much less, and preservation of structures should be better. Bone is efficiently demineralized in ethanolic trimethylammonium EDTA. Retention in the matrix of water-soluble materials (e.g. proteoglycan) was much better than in standard aqueous EDTA demineralization procedures (Scott and Kyffin, 1978).

More detailed decalcification of bone including various decalcifying agents, methods and their effects on bone is described and widely discussed in an excellent review by Callis and Sterchi (1998). Several novel technical approaches to the scanning electron microscopy (SEM) of bone are considered in a paper from Boyde and Jones (1996). These include low kV imaging for the detection of new surface bone packets (and residual demineralized matrix after resorption), low backscattered electron (BSE) imaging of uncoated, embedded, and unembedded samples, environmental SEM for the study of wet tissue, low distortion, very low magnification imaging for the study of cancellous bone architecture, the use of multiple detectors for fast electrons in improving the imaging of porous samples, and high resolution, low voltage imaging for the study of collagen degradation during bone resorption. An SEM study on the process of acid demineralization of cortical bone showed that the interface between the demineralized and mineralized sections of the bone specimens was extremely sharp (Lewandrowski et al., 1997). This study suggests that cortical bone demineralization can be best described using an advancing reaction front theory, and this explanation can be used for implementation of the concept of controlled demineralization (Lewandrowski et al., 1996).

High-resolution AFM imaging of bone (Hassenkam et al., 2004) and electron holography of organic matrixes (Simon et al., 2008) are recently also the subjects of detailed studies.

## 5.2. Dentin and enamel

In the history of demineralization studies, the driving force was based on problems of dental caries (Ehrlich et al., 2008). Dental caries consists of demineralization of the mineral phase, followed by proteolytic degradation of the organic phase (Fig. 8). Initiation of the root caries in the cementum involves sub-surface demineralization (Schüpbach et al., 1989), starting at several

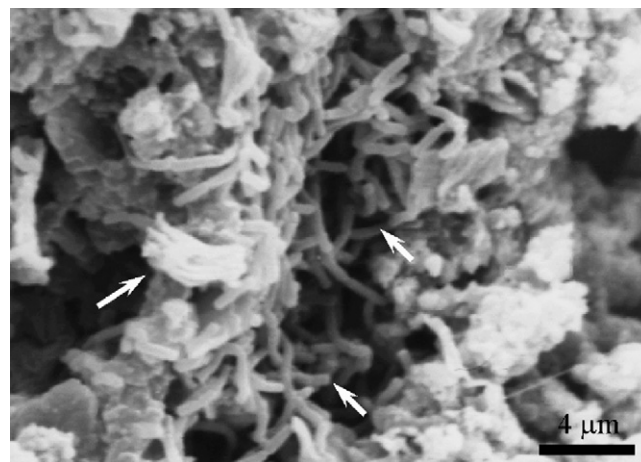


Fig. 8. SEM image: cariogenic bacteria on the work.

points over a wide area of exposed cemental surface. Because cementum is thin and porous, caries rapidly extends to the underlying dentin.

Dentin is a mineralized connective tissue which constitutes the main bulk of the tooth. As in the case of bone, the major structural protein of dentin is type I collagen, the molecules of which are also aggregated into collagen fibrils with an axial period of  $\sim 67$  nm. The apatite crystallites are present in the form of fibrils and they exceed (by weight and volume) the respective bone content (Glimcher, 2006). It is significant to note that dentin contains several highly phosphorylated proteins which, as suggested by *in vitro* experiments with synthetic polymers containing variable amounts of phosphate groups, they are able to induce the formation of hydroxyapatite (Dalas et al., 1990, 1991). Tooth enamel on the other hand is an outer layer of 1–3 mm thickness which covers and protects dentine and pulp cavity. Approximately, 96 wt% of enamel consists of crystalline HAP, the rest of components being the organic matter (*ca.* 0.6%) and water (*ca.* 3.5% by weight) for the mature enamel. The mineral component is reduced upon enamel maturation and may vary in a manner that relates to local conditions and dietary habits (Ten Cate, 1979; Brudevold, 1962). It is interesting to note that the composition of the outer, reactive surface of enamel is different than the bulk composition. Sodium, magnesium, carbonate and fluoride concentrations at the surface exceed those in the bulk enamel (Miles, 1967; Peterson, 1975). In accordance the solubility of the enamel differs significantly, being higher than the corresponding for stoichiometric HAP. The solubility of the outer enamel surface is even lower, a fact which is certainly associated with the different composition and with the presence of  $\text{HPO}_4^{2-}$  (Patel and Brown, 1975). Recent investigations using *in situ* AFM measurements and SEM observation of the apatitic crystallites have shown that enamel demineralization takes place anisotropically along the *c* axis, resulting in hollow enamel cores and nanosized remaining crystallites, resistant to further dissolution (Finke et al., 2000; Lijun et al., 2005). The fact that saliva contains sufficiently high calcium and phosphate concentrations make enamel resistant to demineralization (Dawes and Jenkins, 1962; Schmidt-Nielsen, 1946). It should be noted that saliva is the main “protector” of the teeth in that it is supersaturated with respect to tooth mineral. There are several salivary proteins which inhibit the rate of precipitation of mineral from the supersaturated saliva. Thus there is always a tendency for remineralization to occur because of this supersaturation. In fact, the only reason why the teeth do not enlarge continuously in the mouth is because of the presence of the acquired enamel pellicle on the surface of the teeth. This thin

deposit contains ~130 different salivary proteins and provides a barrier to continued growth of enamel crystals. On pellicle removal by abrasion or attrition, it is rapidly replaced, thus forming a renewable lubricant. When teeth have been subjected to acid erosion, the acid dissolves the surface enamel if the pH of the fluid is less than that at which the fluid becomes unsaturated with respect to tooth mineral. The surface enamel which has been dissolved cannot be regrown because of the blocking action by the rapid deposition of a new acquired enamel pellicle on exposure of the eroded enamel to saliva.

The accumulation of microbial plaque on one hand lowers the pH of the environment in which enamel is exposed and on the other hand causes fermentation of the carbohydrates which results to pH values lower than 5 (Stephan, 1940). The dental plaque or “pellicle” establishes a diffusion barrier for the flux of ions both to the inside and the outside environment. It has been suggested that it is possible for the surface layer to be retained while the subsurface enamel dissolves (Moreno and Zahradnik, 1974; Zahradnik et al., 1976). Investigations on the effect of ionic strength on enamel dissolution have shown that the rates of demineralization were enhanced while the formation of the surface layer was reduced, suggesting diffusive coupling between the acid and the dissolving ions (Anderson et al., 2004). In the oral environment, acid attack may be brought by acids present in foodstuff and drinks (Barbour et al., 2003). Dental caries begins largely as a subsurface lesion underneath a biofilm (dental plaque). While the surface zone of the lesion is intact, the inside of the lesion is sterile and, if the lesion is kept free of plaque, there is the possibility of remineralization, particularly in the presence of fluoride. Dental caries is caused by microbially formed acid in dental plaque. There is still no consensus on the factors maintaining the surface zone of the early lesion. It may, for instance, be due to the deposition of more acidic forms of calcium phosphate, such as dicalcium phosphate dihydrate, as the calcium and phosphate ions leave the enamel. Because of the presence of dental plaque, the calcium and phosphate ions which leave the enamel are not immediately washed away by the oral fluids, as occurs in the process of acid erosion. The dical may then reconvert to hydroxyapatite when the plaque pH rises above the so-called “critical pH”. The latter is defined as the pH at which the plaque fluid (the fluid phase of dental plaque) is just saturated with respect to tooth mineral. It is somewhat lower (about pH 5.1) than the critical pH of saliva, as plaque fluid contains higher concentrations of calcium and phosphate than does saliva.

The mechanism of acidic interaction with HAP was found to involve two phases (Fig. 9) (Yoshioka et al., 2002). In the first phase, carboxylic acids bond to calcium of HAP. Depending on the

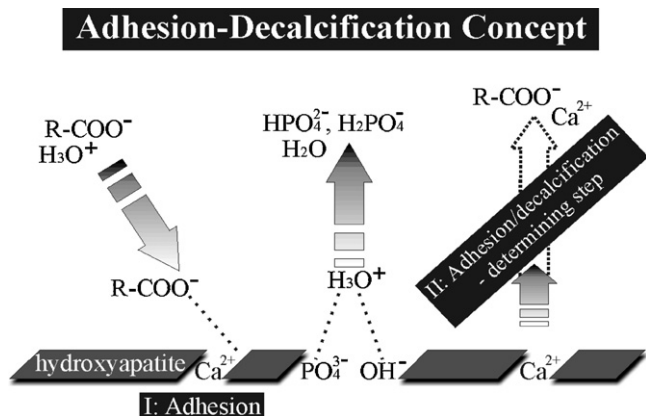


Fig. 9. Schematic presentation of the adhesion/decalcification concept adapted from Yoshida et al. (2001).

diffusion rate of the calcium–acid complexes into solution, the acid will in the second phase either remain attached to the HAP surface with only limited decalcification involved, or the calcium–acid complex will debond, resulting in a substantial decalcification effect. HAP crystallinity was found not to affect the adhesion/decalcification (AD) behavior of different acids when interacting with apatitic substrates, so that the AD-concept can be applied to all human hard tissues with varying HAP crystallinity (Yoshioka et al., 2002).

There are two reasons for the increased solubility of enamel in acid (Dawes, 2003). First, the hydrogen ions remove hydroxyl ions to form water, as follows:  $H^+ + OH^- = H_2O$ . The product of  $[H^+][OH^-]$  in water is always equals  $10^{-14}$  (mol/L). Therefore, as the  $[H^+]$  increase in an acid solution, the  $[OH^-]$  must decrease in a reciprocal manner. Second, the inorganic phosphate in any fluid such as saliva or plaque fluid is present in four different forms, namely  $H_3PO_4$ ,  $H_2PO_4^-$ ,  $HPO_4^{2-}$  and  $PO_4^{3-}$ , and the proportions depend entirely on the pH. Fig. 10 illustrates how the proportions of the four phosphate species vary with pH when the total phosphate concentration is  $5 \times 10^{-3}$  mol/L, as is typical for saliva. The lower the pH, the lower the concentration of  $PO_4^{3-}$ , the only species that contributes to the ionic product of HAP (Dawes, 2003). Thus, as any solution is acidified, the calcium concentration is unaffected but the concentrations of both  $OH^-$  and  $PO_4^{3-}$  are reduced and so, therefore, is the ion product, often to a value less than the solubility product. Dawes (2003) proposed the concept of critical pH for dissolution of enamel in oral fluids. The critical pH is the pH at which a solution is just saturated with respect to a particular mineral, such as tooth enamel. Saliva and plaque fluid are normally supersaturated with respect to tooth enamel because the pH is higher than the critical pH, so our teeth do not dissolve in our saliva or under plaque. Fig. 11 illustrates that above the critical pH, plaque fluid will be supersaturated with respect to HAP, while below the critical level it will be unsaturated. Thus, when plaque pH is below the critical level, caries will tend to occur (Dawes, 2007).

It is established that enamel layers at tooth surfaces are among the hardest biological tissues and have highly mineralized structures exhibiting features that are close to pure synthetic apatites with about 97% mineral phase (Dorozhkin, 2007).

Concentrations of the Four Phosphate Species as a Function of pH

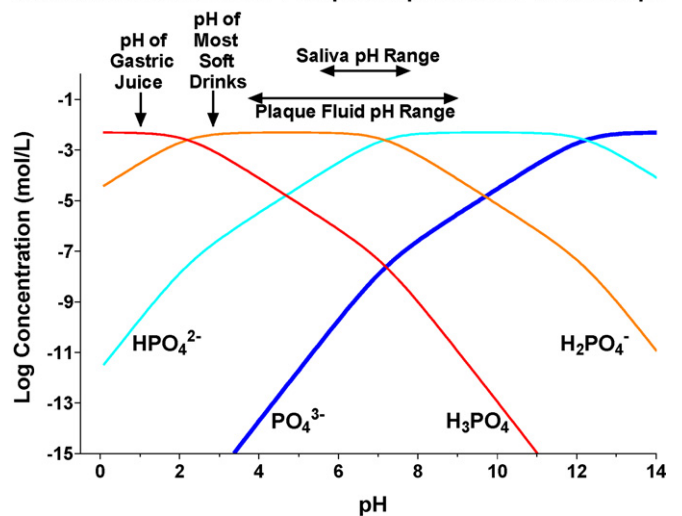
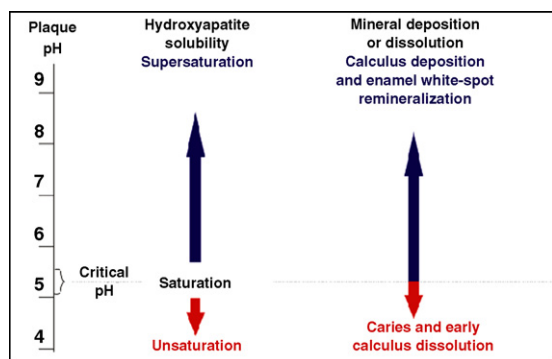


Fig. 10. The effect of pH on the concentrations of the various inorganic phosphate species in saliva containing a total phosphate concentration of  $5 \times 10^{-3}$  mol/L. there is a marked fall in the concentration of  $PO_4^{3-}$  (thick line) as the pH is reduced (adapted from Dawes, 2003).



**Fig. 11.** The effect of plaque pH, which may range from about 4 to 9, on hydroxyapatite solubility and on the tendency for mineral deposition or dissolution. At the critical pH, which varies slightly among individuals, plaque fluid is just saturated with respect to hydroxyapatite and there is no tendency for mineral to deposit or dissolve (adapted from Dawes, 2006).

However, carbonate is always present and although the amount is relatively low, the substitution of carbonate to phosphate ions in the apatite crystal lattice results in a contraction of the *a*-axis and expansion of the *c*-axis dimensions of the unit cell, as well as a decrease in crystallinity and increase in solubility and acid reactivity. Under physiological conditions, the suppression of tooth enamel surface dissolution is much more marked and the demineralization only takes place at relatively high undersaturations ( $\sigma > 0.4$ ) and at lower pH ( $< 5.5$ ) (Tang et al., 2004a). Even at higher saturations of  $\sigma = 0.90$ , the demineralization rate of tooth enamel surfaces is extremely slow and complete dissolution requires about 4 weeks. It was reported, that the surface of enamel prior to dissolution is composed of numerous needle-like apatites at an approximately micrometer scale (Tang et al., 2004a). However, complete dissolution of the inorganic particles does not take place, rather, the apatite sizes decrease and nano particles are formed. This phenomenon is due to the formation and spreading of active etch pits on the dissolving surfaces. Only when the pits are larger than a critical size, do they contribute to dissolution. It is found by Nancollas and co-workers that the dissolution can be self-inhibited and even suppressed due to decreasing crystallite size (Wang et al., 2005). Biomaterials become insensitive to dissolution in undersaturated solutions and may be stabilized in the fluctuating biological milieu. An excellent example is proposed by Tang et al. (2004b) in studies of caries lesion formation. Enamel surfaces remain undissolved in water (pH 5.5–5.8) in spite of the undersaturation. Caries (dissolution) is only induced at localized sites where bacteria have produced acidic conditions. The mineral crystallites can be stabilized in the fluctuating physiological fluids, thus exercising a degree of self-preservation as the result of this kinetic size-effect at the nanoscale level.

The chemistry of enamel caries, kinetics and mechanisms of dental enamel demineralization were discussed in detail in special reviews and experimental papers (e.g. Fosdick and Hutchinson, 1965; Thylstrup et al., 1994; Robinson et al., 2000; Oliveira et al., 2002; Anderson et al., 2004; Hannig et al., 2005).

Various electron microscopy techniques were used for detailed observation of dentinal demineralization on nano- and micro-levels. Comparative SEM studies focused on the effect of different demineralization methods on dentin surfaces (Isik et al., 1997), and on microbial contamination of noncavitated caries lesions (Parolo and Maltz, 2006). High-resolution electron microscopy (HR-TEM) was used in investigations on mechanism of the dimensional increase in demineralized dentine crystals (Hayashi et al., 1997). More recently Yanasigawa and Miake (2003) employed HR-TEM to

demonstrate demineralization and remineralization of enamel crystals obtained from cross-cut sections of the *c*-axis of crystals from carious lesions. Atomic force microscopy (AFM) was widely used in the examination of the early stages of acid treatment of dentin (Marshall et al., 1993), and of food-induced demineralization of the tooth enamel (Finke et al., 2000). AFM based nanoindentation has been used to study the nanomechanical properties and the ultrastructure of enamel samples as affected by demineralization/remineralization cycles (Lippert et al., 2004). High-resolution AFM was also successfully used in studies on sequential demineralization and deproteinization of dentin with respect to investigations of partially demineralized human dentin collagen fibrils (Habelitz et al., 2002).

### 5.3. Corals

Corals are phylogenetically basal metazoans, possess a simple anatomy, can be easily manipulated for physiological studies, and possess a majority of genes in common with vertebrates (Tambutté et al., 2007). They are therefore good models for biochemical, physiological, and evolutionary studies concerning either the transport of ions or synthesis of organic matrix involved in biomineralization processes. Demineralization of coral skeletons using different techniques and chemical agents leads to isolation of the following biomacromolecules as reported in literature: chitin (Wainwright, 1963), collagens (Kingsley et al., 1995; Franc et al., 1985), gorgonin (Ehrlich et al., 2006; Noé and Dullo, 2006; Sherwood et al., 2006), canthaxanthin (Cvejić et al., 2007) and a wide diversity of proteins (reviewed in Tambutté et al., 2007).

Scleractinians (stony corals) are a group of calcified anthozoan corals, many of which populate shallow-water tropical to subtropical reefs. Most of these corals calcify rapidly and their abundance on reefs is related to a symbiotic association with zooxanthellae. These one-celled algal symbiots live in the endodermal tissues of their coral host and are thought responsible for promoting rapid calcification (Stanley, 2003). Recently, Fine and Tchernov (2007) presented an experimental approach documenting how coral skeletons dissolve as a physiological response to increased atmospheric  $\text{CO}_2$ . Thirty coral fragments from the five coral colonies of the scleractinian Mediterranean species were subjected to pH values of 7.3–7.6 and 8.0–8.3 (ambient) for 12 months. The corals were maintained in an indoor flow-through system under ambient seawater temperatures and photoperiod. After 1 month in acidic conditions, morphological changes were seen, initially polyp elongation, followed by dissociation of the colony form and complete skeleton dissolution. Surprisingly, after 12 months, when transferred back to ambient pH conditions, the experimental soft-bodied polyps calcified and reformed colonies.

It should be noted that the organic matrix of scleractinian corals can be divided into “soluble” and “insoluble” components (Weiner, 1984) depending of the extraction method used, and consequently care must be taken when comparing and interpreting results. Moreover, in 1980, Johnston (Johnston, 1980) warned that a differentiation should be made between “skeletal organic matrix” and “skeletal organic material”, and suggested that the latter involved the skeletal organic matrix plus all other contaminating components such as endoliths and trapped tissues. From that time, in order to avoid such contamination, the chemical treatment of corals was carefully performed on the powders of skeletons (usually created using sodium hydroxide and/or bleach) in order to obtain only the skeletal organic matrix. Typical procedure is described by Cuif et al. (1999) in their study on 24 species of corals collected in very various environments, ranging from cold and/or deep seas to tropical lagoons of Polynesian atolls. Coral samples

were thoroughly cleaned with sodium hypochlorite, rinsed, and oven dried (40 °C) overnight. Dried skeletal fragments were powdered. The resulting powder was calibrated to regulate the decalcification process made in very standardized conditions. To carry out the full sequence of mineralizing matrix characterizations, 3 g of the calibrated powder were dispersed in 25 ml of Milli-Q water (magnetic stirring), then decalcification was made by addition of ultra-pure acetic acid under permanent control of the pH. After the complete dissolution of the mineral phase, a low-speed centrifugation allowed soluble and insoluble matrices to be separated. Desalting of soluble components was done on Sephadex G25 gel-based low-pressure standard system, allowing salt and organic compounds of lower molecular weights to be removed. To obtain reliable biochemical information, these two successive steps of preparation play a major role, allowing removal of most of the external contaminants, both insoluble (i.e. possible remains of fungal or algal cell membranes) and low-weight soluble compounds that could have been introduced by seawater flow through coral skeletons (Cuif et al., 1999). Similar decalcification method was described recently for scleractinian coral *S. pistillata* (Puverel et al., 2005a). Microcolonies of this coral species were cleaned by removing soft tissues with 1 M NaOH at 70 °C. The skeletons were then rinsed with ultrapure water, dried at 60 °C overnight, and ground to a fine powder with a mortar and pestle. The powder was resuspended in ultrapure water and decalcified by adding ultrapure acetic acid up to pH 4.0 in the presence of protease inhibitors. After complete dissolution of aragonite, soluble and insoluble matrices were separated by centrifugation (10 min, 10,000 × g). To desalt soluble components, the supernatant containing the soluble organic matrix was ultrafiltered and then lyophilized. Using antibodies raised against soluble organic matrix isolated from coral *S. pistillata* as described above, the authors presented direct evidence for the role of calicoblastic cells in organic matrix synthesis and secretion. The same decalcification method was used in comparative study on *S. pistillata*, known as branched robust coral and *Pavona cactus*, a leafy complex coral (Puverel et al., 2005b). Soluble organic matrix of both coral species were shown to contain high amounts of potentially acidic amino acids and glycine. However, proportions of glycosaminoglycans and SDS-PAGE analysis of soluble organic matrix proteins were very different. Internal peptide sequences of two matrix proteins (one from each species) were obtained. One sequence of *S. pistillata* is unusual because it contains a long poly-aspartate domain, as described in proteins belonging to the calsequestrin family and in proteins from molluscan species.

In contrast to the usual view of an aggregate of purely mineral units (the coral fibres) independently growing by a simple chemical precipitation (Perrin, 2003), coral skeletons appear to be biochemically controlled structures. Different kinds of proteins which are responsible for biomineralization phenomenon were isolated from scleractinian corals. Thus, Cuif and Dauphin (2004) reported on isolation of sulfated acidic proteoglycans which were able to create polymeric frameworks. Atomic force microscopy confirms the close relationship of this organic phase and mineral phase at the nanometric scale. Whereas acidic macromolecules are known to be associated with the mineral phase of Scleractinian coral skeletons (reviewed in Tambutté et al., 2007), galaxin, a matrix protein from the exoskeleton of the zooxanthellate coral *G. fascicularis*, is rich in cystine, serine, glycine and alanine and does not contain high fractions of acidic amino acids (Fukuda et al., 2003).

Previous studies of coral biomineralization strongly focused on scleractinians (see references above), whereas the organic matrix-mediated calcification mode of the soft corals, or Octocorallia, including different alcionarian and gorgonian families is largely

unknown. In contrast to deep-water scleractinians, the slow-growing skeletons of gorgonian octocorals with a longevity potential on the order of hundreds of years form on sub-annual to centennial time scales and hence represent potential archives of past oceanic and climatic dynamics in intermediate and deep-water masses (Noé and Dullo, 2006).

Recently, Rahman and Isa (2005) documented demineralization procedure for spicules of soft coral *Lobophytum crassum* (Rahman and Isa, 2005). The colony of the corals was cut using sharp scissors into small pieces. The pieces were ground five to six times with a mixer machine and washed with tap water until the spicules were obtained. The collected spicules were stirred vigorously in 1 M NaOH for 2 h to remove the fleshy tissues and debris. The mechanically and chemically cleaned spicules were extensively washed in distilled water and decalcified in 0.5 M EDTA (pH 7.8) overnight. The decalcifying solution was centrifuged with 4000 rpm (15 min) to remove any insoluble materials followed by filtration with filter paper. The authors reported that soluble organic matrix comprised 0.03% of the spicule weight. The SDS-PAGE analysis of the preparation showed four protein bands. The 67-kDa protein appears to be glycosylated. Moreover, the isolated organic matrix possesses carbonic anhydrase activity which functions in calcium carbonate crystal formations, indicating that organic matrix is not only structural protein but also a catalyst.

The scleroprotein gorgonin plays a crucial role in the formation of organic nodes and the secretion of calcitic internodes by providing a structural framework in the biomineralization processes (Noé and Dullo, 2006). The decalcification procedure by Osteosoft™ (Merck) treatment was used by Ehrlich et al. (2006) to gain understanding of the nature and nanostructure of the gorgonin-containing organic matrix of octocoral *Isidella* sp. On the 7th day of decalcification at 37 °C authors observed only the presence of a transparent gelatinous pellicle after complete dissolution of the calcite based axis internode of the coral (Fig. 12A and B). Gorgonin layers appear brownish in light microscopy (Fig. 12B) and differ drastically from the transparent organic matrix. The identification of the gorgonin-free organic matrix by means of SEM, TEM (Fig. 12C and D) and AFM (Fig. 13) shows fibrillar protein behaviour. The results of amino acid analysis of this organic matrix show glutamine and proline (28.9 and 24.0%, respectively) as the dominant components among other amino acids detected. The very low content of glycine (2.5%) rules out the possibility of the fibrillar matrix being of a collagenous nature. It was concluded (Ehrlich et al., 2006) that isolated structural protein is an example of an acidic fibrillar protein. This protein was responsible for calcification phenomenon in Isididae corals in contrast to gorgonin-based structural layers on which no mineral phase formation were observed.

Unfortunately, the properties of coral as implants have generally been studied with non-demineralized skeletons rather than with whole extracts of organic matrix or isolated molecules. Since in coral larvae and adults, the molecules involved in mammal osteogenesis such as bone morphogenetic proteins (BMPs) are present in tissues (Hayward et al., 2002), the study of such ancestral molecules and their potential implications in coral skeleton formations, as well as in mammalian osteogenesis, might open new pathways not only in medicine but also in evolutionary studies of biomineralization.

#### 5.4. Crustacea

Crustaceans are a remarkable group of animals because of their ability to elaborate cyclically two kinds of calcified biomineralizations: an unstretchable exoskeleton (or cuticle) and also, for many species, depending of the way of life of the considered animal,

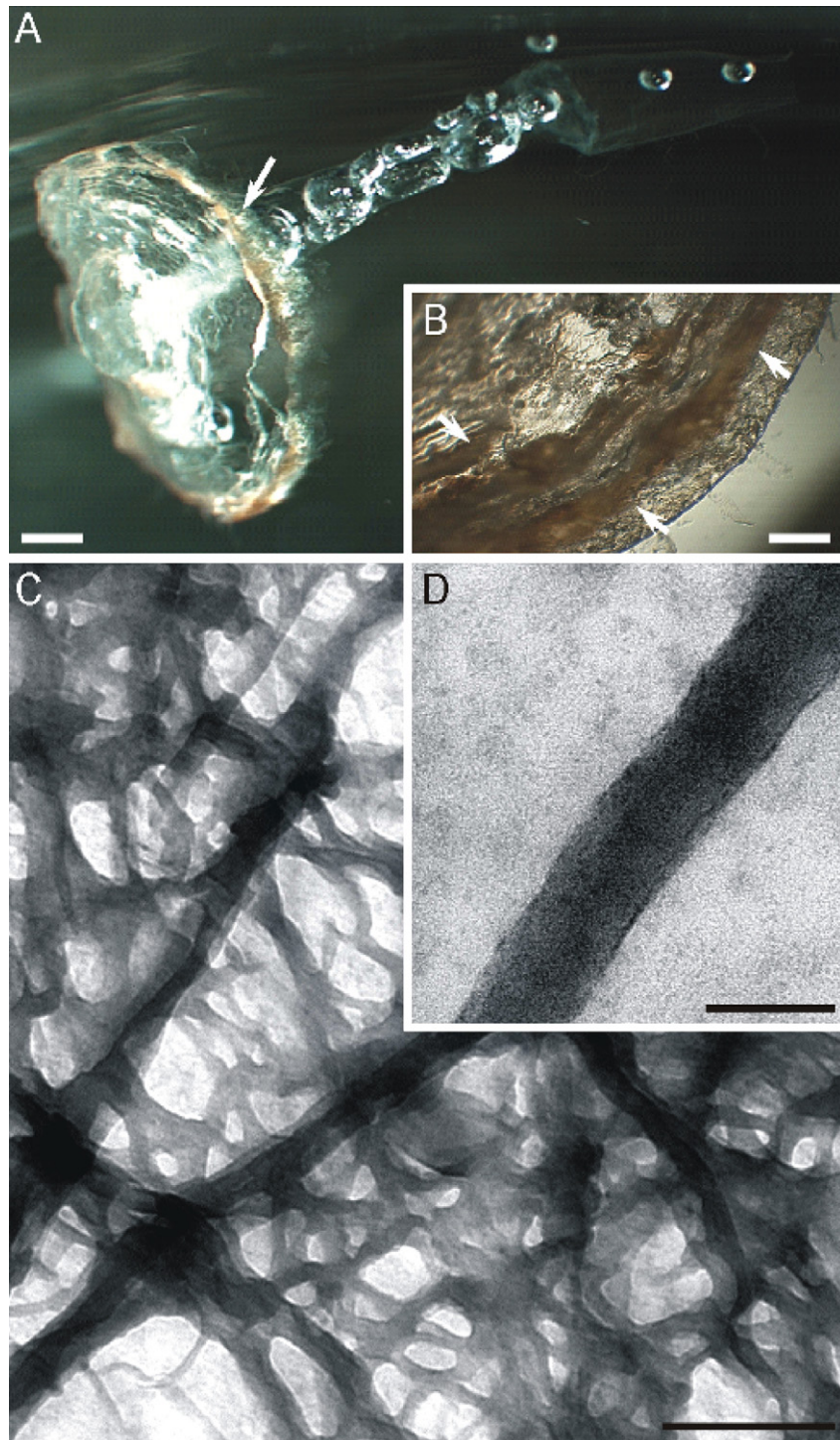


**Fig. 12.** Light microscopy image of organic matrix isolated from *Isidella* sp. octocoral using Osteosoft-based demineralization technique at 37 °C (A). Brownish coloured layers of gorgonin which is resistant to calcification could be visualized under magnification of the same sample (B). Nanoorganised structures made by acidic fibrillar protein responsible for mineralization of octocoral skeletal internodes are observed using TEM (C and D).

transitory calcium deposits (Luquet and Marin, 2004). They serve as an ideal model for the study of calcium homeostasis due to their natural molting cycle. Demineralization and remineralization of the calcified cuticle is accompanied by bidirectional  $\text{Ca}^{2+}$  transfer across the primary  $\text{Ca}^{2+}$ -transporting epithelia: gills, antennal gland (kidney), digestive system, and cuticular hypodermis (Wheatly, 1999).

The major sources of  $\text{Ca}^{2+}$  for crustaceans are water and food, with water being the most important in zooplankton. Develop-

ment and associated growth force crustaceans to replace their cuticle frequently. During ecdysis, most of the  $\text{Ca}^{2+}$  is lost with the residual exuvia and must be replaced by absorption of the mineral from the environment (Fabritius and Ziegler, 2003). Most of the  $\text{Ca}^{2+}$  is probably associated with carbonate and phosphate minerals in the carapace (Stevenson, 1985), because calcification is the primary cause of hardening in crustaceans cuticles (Chockalingam, 1974). However, freshwater decapods may store some 20–30% of  $\text{Ca}^{2+}$  on the form of gastroliths (Wheatly and

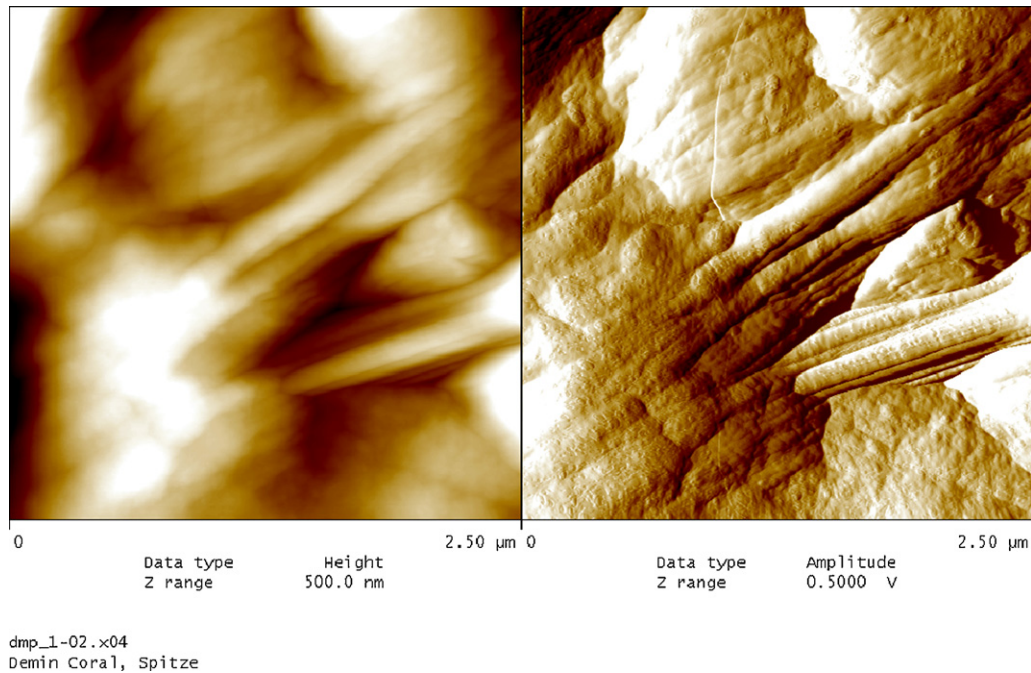


**Fig. 13.** AFM imaging of the *Isidella* sp. octocoral fibrillar organic matrix isolated after decalcification.

Ayers, 1995). While it is easy for marine, and to a lesser degree for limnic species to replace  $\text{Ca}^{2+}$  by taking it up from the water via their gills, terrestrial crustaceans depend on  $\text{Ca}^{2+}$  taken up with their diet, which contains little  $\text{Ca}^{2+}$  (Fabritius et al., 2005). Terrestrial isopods store  $\text{Ca}^{2+}$  in a variety of storage sites, the most common among these are the sternal  $\text{CaCO}_3$  deposits located within the ecdysial gap between the epithelium and the old cuticle of the first four anterior sternites (Ziegler and Miller, 1997). The storage amounts of  $\text{Ca}^{2+}$  are highly variable in different crustaceans. For example, semiterrestrial *Ligia* spp. seems to have the highest  $\text{Ca}^{2+}$ -storage capability (about 75%) among crustaceans in general (Ziegler et al., 2007). Terrestrial amphipods store 67% of their  $\text{Ca}^{2+}$ , the freshwater/land crab *Holthuisana transversa* 64%, various land crabs 5–14%, and freshwater crayfishes about 17% (reviewed in Ziegler et al., 2007).

The majority of the skeletal structures of crustaceans are composed of calcium carbonate in the form of calcite (Romano et al., 2007), francolite, a carbonate containing F-apatite (Löwenstam, 1971; Watabe and Pan, 1984), and amorphous calcium carbonate (ACC) (Fabritius et al., 2005), or amorphous calcium phosphate (Raz et al., 2002). In all cases mineral phases are associated with an organic matrix (chitin and/or proteins), suggesting that the organic components function as a template for biomineralization in crustaceans.

In contrast to studies on demineralization of skeletons in other invertebrates, the main driving force in the case of crustaceans is determined by the practical applications of chitin. Recovery of chitin from shells of crustacean species is desirable in many locations throughout the world where shrimps, prawns, lobsters, crab, crayfish, etc. are harvested. One of the difficulties in processing crustacean shells to recover chitin, is the removal of the large amounts of mineral matter, primarily calcium carbonate. Historically, chitin has been isolated from crustacean shell by boiling the shell with strong caustic alkali solutions to remove protein and dissolving away the mineral matter with strong mineral acid, usually hydrochloric acid (Allan et al., 1978). In 1948 Max Lafon described the demineralization procedure of crustacean integument as follows (Lafon, 1948). The integument is carefully

freed of the hypodermal layer by scrapping, then rapidly washed, dried and ground to very small fragments, dried and weighed. It is then demineralized by treatment for 24 h in the cold with 2% HCl. It was shown that the proteins are unaltered by this treatment. After demineralization, the hydrochloric acid solution is removed by filtration, the organic matter is washed twice rapidly and the wash waters are removed. The demineralized integument is next extracted with a buffer solution at pH 9.2 consisting of borax solution (19 g/L), 5 parts; water, 5 parts; 95% ethanol, 4 parts; ether, 1 part for 36 h at 55 °C. The residue was next extracted with 5% sodium hydrochloride solution for 5 h at 55 °C and then 1 h at 100 °C. This removed all of the less soluble protein leaving essentially pure chitin as a final residue. It should be recognized that Lafon's extraction medium for the more soluble protein was intended for research purposes and is not practical for a commercial process. Also, his use of 5% NaOH at 100 °C is too drastic for production of a protein of good nutritional value.

As an alternative to the chemical process, a biological process has been evaluated for deproteination and demineralization. Lactic acid bacterial fermentation for demineralization has been reported for shrimp waste, crayfish exoskeleton, scampi waste, prawn waste and red crab shell waste (as reviewed in Jung et al., 2005). Successive two-step fermentation was carried out from red crab shell wastes for biological extraction of chitin in combination of the 1st step with a lactic acid bacterium *Lactobacillus paracasei* subsp. *tolerans* KCTC-3074 and the 2nd step with a protease producing bacterium *Serratia marcescens* FS-3, and vice versa. The successive fermentation in the combination of both strains gave the best result in co-removal of  $\text{CaCO}_3$  and proteins from crab shells. In this combination, the rates of demineralization and deproteination were 94.3% and 68.9%, respectively, at the end of fermentation (Jung et al., 2007).

Crustacean's cuticle is also a good example of biological structures with hierarchical organization from the nanometer to the millimetre scale. Recently, Raabe and co-workers published several impact papers regarding to microstructure and crystallographic texture of the chitin-protein network in the biocomposite material of the exoskeleton of different crustaceans including

lobster *Homarus americanus* (Raabe et al., 2005a,b; Sachs et al., 2006; Raabe et al., 2006; Romano et al., 2007). The following demineralization procedure was used in these experiments. Samples of the exoskeleton of an American lobster were cleaved either perpendicular to the cuticle surface to expose the cross-section or parallel to the surface to expose the endocuticle. The cleavage was done prior to chemical attack to avoid the formation of structural artefacts. Chemical attacks were performed using NaOH (1 M, 1 week) to remove the protein structure, EDTA (0.15 M, 2 weeks) to remove the biominerals and a combination of EDTA (0.15 M, 2 weeks) followed by NaOH (1 M, 1 week) to obtain only the chitin network (Romano et al., 2007). The results obtained showed that chemical treatment had a severe impact on the lobster cuticle microstructure (Fig. 14). During decalcification with EDTA the  $\text{CaCO}_3$  was gently removed and the remaining structure was formed by chitin-protein fibers, which themselves are composed of protein-wrapped nanofibrils. The smoothness of the structure without  $\text{CaCO}_3$  is in contrast to the blocky appearance of the untreated cuticle, indicating that the biominerals were indeed located between and around the chitin-protein fibers. The absence of structural roughness caused by the removal of the minerals also shows that the chemically treated material loses the brittleness present in the natural state. It was also reported, that in lobster cuticle proteins stabilize not only the structure but the crystalline state by binding the mineral together with the chitin polymer (Romano et al., 2007).

The protein and glycoprotein content of four different neutral or acidic solvents extracts (0.5 M KCl, 10% EDTA, 0.1N HCl, or 2% acetic acid) from the mineralized exoskeleton of a decapod crustacean, the Atlantic shore crab *Carcinus maenas*, were characterized by quantitative analysis of proteins, SDS-PAGE analysis, and probing with lectins on blots (Compere et al., 2002). The results show that many of the extracted cuticle proteins appeared to be glycosylated, bearing O-linked oligosaccharides and N-linked mannose-rich glycans. N-Acetyl-galactosamine and N-acetylneuraminic acids were revealed, for the first time, as terminal residues on N-linked mannose-rich structures of crab cuticle glycoproteins. Sialylated glycoproteins might thus be involved in organic-mineral interactions in the calcified crab exoskeleton. The amount and variety of glycoproteins extracted with the acidic solvents are obviously different from those extracted with neutral solvents. The authors reported that HCl proved to be the best of the tested extraction solvents and a valuable alternative to EDTA.

The atremate brachiopods are unique in that they possess shells of calcium phosphate and concentrate relatively high amounts of fluoride in their skeletons. In *Lingula adamsi* and *Glottidia pyramidata*, the shell mineral is  $(\text{CO}_3^{2-} + \text{F}^-)$ -containing apatite and is crystallo-chemically similar but not identical to the mineral francolite (Watabe and Pan, 1984). The average F content determined by electron probe analysis is 1.64 wt% of whole shells and 2.58% of highly calcified layers. The crystallinity of the brachiopod shell apatite is greater than that of human dentine but less than that of mammalian enamel. The authors reported about two types of organic matrices which are present in the primary and mineralized layers of brachiopods shells. One is a protein matrix in the form of fibers, approximately by 5 nm in diameter and is demonstrated by simultaneous decalcification and staining of thin sections with uranyl acetate. The other is the glycosaminoglycan (GAG) matrix which becomes evident in thin sections of shells fixed with glutaraldehyde containing acridine orange. The GAG matrix is also fibrous, 5 nm in diameter and forms a fine network surrounding the apatite crystals. The close association of the GAG matrix with the apatite nanocrystals may suggest its significant roles in crystal formation and growth (Watabe and Pan, 1984).

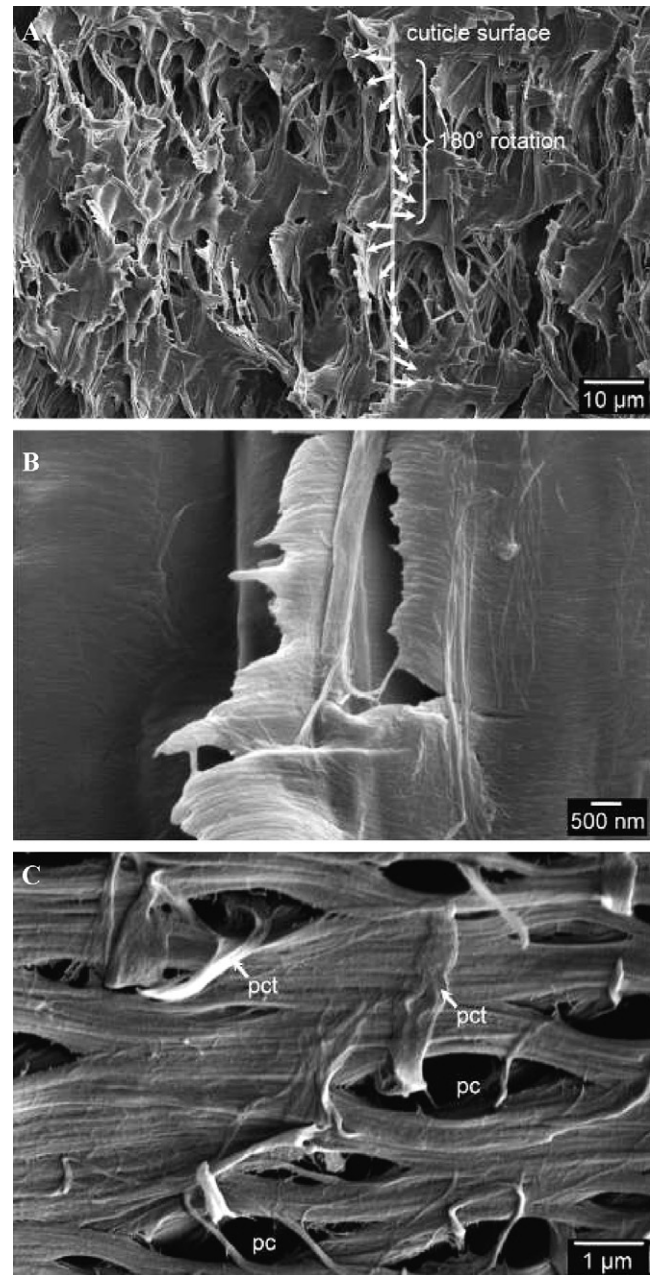


**Fig. 14.** (A) SEM micrograph of demineralized and deproteinated (0.15 M EDTA, 2 weeks + 1 M NaOH, 1 week) cuticle of the American lobster *Homarus americanus*. The cross section shows the typical twisted plywood structure of the horizontal chitin fibre layers (arrows) arranged around longitudinally fractured pore canals. (B) Detail image showing stacked individual fibers of purified chitin in and a cut pore canal in lobster cuticle. (C) SEM micrograph of demineralized and deproteinated (0.15 M EDTA, 2 weeks + 1 M NaOH, 1 week) cuticle of *Homarus americanus* fractured parallel to the surface. The chitin fibres are arranged around the cavities of the pore canal (pc) system resulting in a honeycomb-like structure. The pore canals contain fibres oriented perpendicular to the twisted plywood structures originating from the pore canal tubes (pct).

Calcium storage structures in crustaceans are calcareous concretions which are formed essentially of amorphous calcium carbonate, precipitated within an organic matrix synthesized by the storage organ cells (Graf, 1967; Hecker et al., 2004). It was suggested, that stabilization of these amorphous minerals in crustaceans is probably due to macromolecular constituents of the organic matrix, and to the magnesium and phosphate present in the mineral phase (Raz et al., 2002).

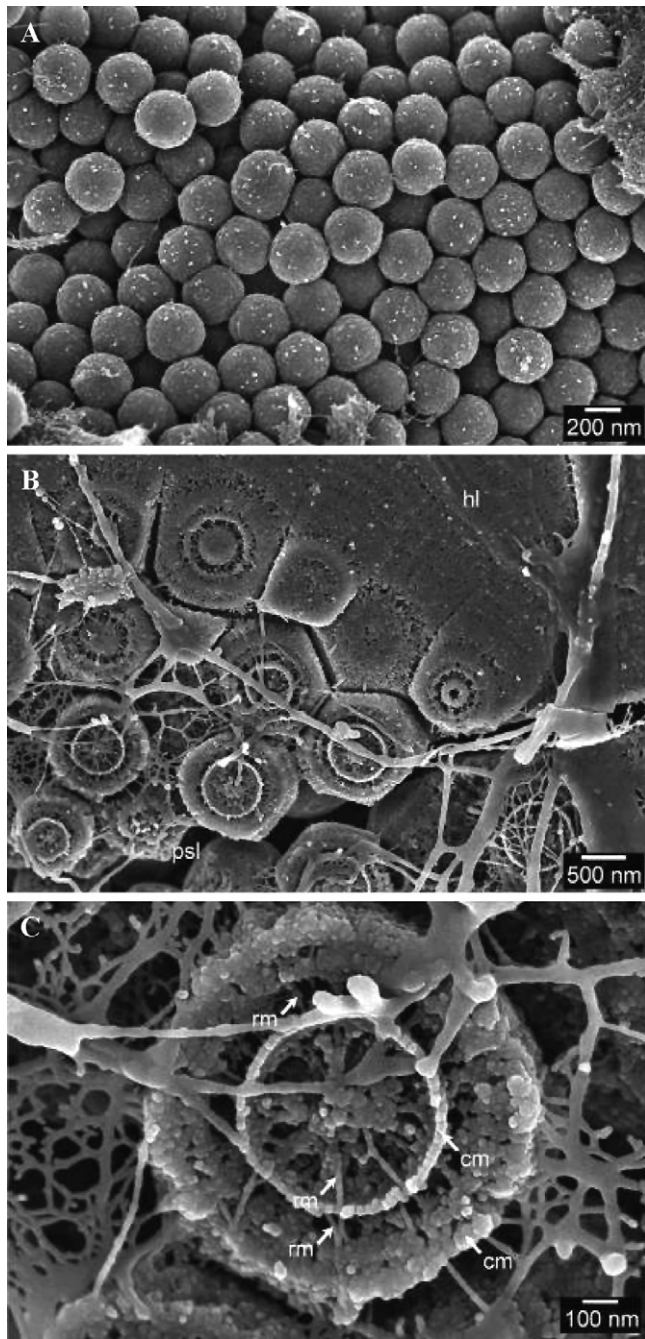


**Fig. 15.** (A) Untreated spherules in the proximal spherular layer in fully developed sternal ACC deposits of *Porcellio scaber* in late premolt stage. Material consists of ACC-nanoparticles associated with fibrillar matrix structures which display different states of dissolution. (B) SEM micrograph of sagittally cut fully developed sternal ACC deposits of the woodlouse *P. scaber* in late premolt stage. The sample surface has been polished using an ultra-microtome followed by decalcification in 0.1 M EDTA with 2.5% glutaraldehyde for 10 min. The image from the transition zone between the proximal spherular layer (psl) and homogeneous layer (hl) shows the results of demineralization. (C) High resolution SEM micrograph of a single cross sectioned spherule consisting of several concentric matrix reticules (cm) still associated with undissolved ACC-nanoparticles which are connected by radial matrix filaments (rm).

*Orchestia cavimana* is a terrestrial amphipod that provides a dramatic example of calcium storage process with respect to formation of amorphous calcium carbonate phase which is localized within an organic matrix synthesized by a caecal epithelial cells in the lumen of posterior caeca. After extraction

of the organic matrix in a buffer containing EDTA, electrophoretic analysis of the proteinaceous components led to reveal about 11 polypeptides in the EDTA-soluble fraction. Among them, an acidic polypeptide migrating at 23 kDa in SDS-PAGE appeared specific to the EDTA-soluble fraction organic matrix. Sequencing and characterization of this protein, called Orchestrin, revealed that it is the only organic matrix component able to bind calcium and it is phosphorylated (Hecker et al., 2003). Recently, Marin and Luquet (2007) reported about occurrence of unusually acidic proteins (with *pI* below 4/4.5) isolated from crustaceans skeletal formations. Thus, for crustaceans, 28 complete cuticular protein sequences (plus nine partial sequences) have been retrieved. In addition, two complete protein sequences of calcium storage structures have been determined. From these 30 sequences, 21 can be considered as unusually acidic.

Recently, Fabritius et al. (2005) presented results of a detailed ultrastructural investigation of the organic matrix of the sternal  $\text{CaCO}_3$  deposits of terrestrial crustacean *P. scaber* using high-resolution field-emission scanning electron microscopy. In *P. scaber* 10–30 nm thick amorphous calcium carbonate nanoparticles occur in mature spherules and on the surface of forming and degrading spherules. The authors showed that these nanoparticles are often preserved in some of the concentric layers and at the surface of radial strands of the organic matrix (Fig. 15). These particles must be stabilized to a higher degree than the in EDTA dissolved material between radial strands and some concentric layers. It is of interest that similar particles have been described along rod-like chitin-protein fibres in the exo- and endocuticle of the crab *Carcinus maenas* (Roer and Dillaman, 1984). Although the main mineral phase in the mature cuticle of decapods is calcite, ACC occurs in premolt cuticles suggesting that the calcitic nanoparticles in the cuticle originate from amorphous precursors.

Gastroliths are calcified structures formed in the cardiac stomach wall in crustaceans (Luquet and Marin, 2004). They appear as paired discs in some decapods such as crayfishes, lobsters and as four more irregular concretions in gecarcinid land crabs. Nagasawa and co-workers described solubilization technique of gastrolith matrix protein (GAMP) (Ishii et al., 1996, 1998; Takagi et al., 2000). Gastroliths were collected from the crayfish 7–10 days after bilateral eyestalk ablation. The gastroliths were immersed in 1 M acetic acid for two days. After the decalcifying solution was poured off, the residue was washed with distilled water several times. Then the residue was extracted separately with mixtures of one or more of three solutions, 6 M urea, 1% SDS, and 10 mM dithiothreitol, in various combinations at 100 °C for 10 min. Each extract was digested with trypsin to check whether the GAMP fragment was generated or not. Finally, an insoluble matrix protein, referred to as gastrolith matrix protein, was made soluble with 1% SDS containing 10 mM dithiothreitol, and was purified by reverse-phase high-performance liquid chromatography. The protein had a molecular weight of about 50,500 and a blocked amino terminus. The GAMP fragment has a tandemly repeated sequence not reported before; each repeat consists of five amino acid residues. X-ray analysis showed that calcium carbonate in the gastrolith was amorphous, whereas that in the exoskeleton consisted of calcite (Takagi et al., 2000).

## 6. Epilogue

It is apparent that decalcification is an intricately complex mechanism that serves several purposes, from organisms' survival to structural protection to calcium balance. Since centuries ago, man's curiosity has been the driving force to delineate the mechanisms involved in (either "natural" or "pathological") decalcification. Several scientific fields can benefit from knowing

natural decalcification mechanisms. For example, calcium-containing deposits are known as significant problems in process water systems (Demadis et al., 2005, 2006). These can be decalcified/dissolved by the action of a variety of  $\text{Ca}^{2+}$  chelating molecules. It is apparent that decalcification and calcification should be envisioned as the two sides of the same coin. Nature often uses these in admirable synergy to achieve a multitude of purposes. Continued advances in instrument technology will make it possible to further untangle unresolved issues. There is a plethora of opportunities for innovative research and applied science. In particular, applications centered around human health and well-being are the main drivers forward.

## Acknowledgements

Authors would like to acknowledge Prof. S. Weiner, Prof. M. Ilan (Israel); Prof. M. Glimcher, Prof. H.C. Skinner, Prof. G. Nancollas, Prof. D. Morse, Prof. S. Golubic, Prof. Henry L. Ehrlich, Prof. A. George, Prof. G. Marshall, Prof. A. Lüttge, Prof. C. Pueschel, and G. Callis (USA); Prof. C. Dawes (Canada); Prof. G. Gadd, Prof. J. Elliott, Dr. M. Barbour (UK); Prof. Y. Dauphin, Prof. J.P. Cuif, Prof. J. Vacelet, Prof. G. Luquet (France); Prof. D. Allemand (Monaco); Prof. K.D. Jandt, Prof. M. Epple, Prof. W.E.G. Müller, Prof. G. Wörheide, Prof. E. Bäuerlein, Prof. B. Schöne, Prof. H. Worch, Prof. D. Raabe, Prof. R. Kniep, Dr. P. Simon, Dr. A. Ziegler, Dr. C.H. Schönberg, Dr. H. Fabritius, Dr. M. Wisshak, Dr. S. Noe (Germany); Prof. E. Königsberger (Australia); Dr. S. Dorozhkin (Russia) for discussion and comments. We wish to thank Vasily V. Bazhenov for excellent technical assistance.

This work was supported by German Research Foundation (DFG) grant WO 494/17-1, and the General Secretariat of Science & Technology, Greece.

## References

- Ackerman, J.L., Raleigh, D.P., Glimcher, M.J., 1992. Phosphorus-31 magnetic resonance imaging of hydroxyapatite: a model for bone imaging. *Magnetic Resonance in Medicine: official journal of the Society of Magnetic Resonance in Medicine. Soc. Magn. Reson. Med.* 25 (1), 1–11.
- Alexanderson, E.T., 1975. Marks of unknown carbonate-decomposing organelles in cyanophyte borings. *Nature* 254, 237–238.
- Allan, G.G., Fox, J.R., Kong, N., 1978. Marine polymers. Part 8: a critical evaluation of the potential sources of chitin and chitosan. In: *Proc. Int. Conf. Chitin. Chitosan*, vol. 1. pp. 64–78.
- Amaechi, B.T., Higham, S.M., Edgar, W.M., 1999. Factors influencing the development of dental erosion *in vitro*: enamel type, temperature and exposure time. *J. Oral Rehabil.* 26, 624–630.
- Anderson, P., Bollet-Quivogne, F.R.G., Dowker, S.E.P., Elliott, J.C., 2004. Demineralization in enamel and hydroxyapatite aggregates at increasing ionic strengths. *Arch. Oral Biol.* 49, 199–207.
- Ankel, W.E., 1937. Wie bohrt *Natica*? *Biol. Zentr.* 57, 75–82.
- Arends, J., Jongebloed, W.L., 1977. Mechanism of enamel dissolution and its prevention. *J. Biol. Buccale* 5, 219–237.
- Barbour, M.E., Parker, D.M., Allen, G.C., Jandt, K.D., 2003. Enamel dissolution in citric acid as a function of calcium and phosphate concentrations and degree of saturation with respect to hydroxyapatite. *Eur. J. Oral Sci.* 111, 428–4330.
- Bayrak, B., Laçin, O., Bakan, F., Saraç, H., 2006. Investigation of dissolution kinetics of natural magnesite in gluconic acid solutions. *Chem. Eng. J.* 117, 109–115.
- Belanger, L.F., Copp, D.H., Morton, M.A., 1965. Demineralization with EDTA by constant replacement. *Anat. Rec.* 153, 41–48.
- Birkedal-Hansen, H., 1974. Kinetics of acid demineralization in histologic technique. *J. Histochem. Cytochem.* 22, 434–441.
- Blake, J.A., Evans, J.W., 1973. *Polydora* and related genera as borers in mollusc shells and other calcareous substrates (Polychaeta: Spionidae). *Veliger* 15, 235–249.
- Boquet, E., Boronat, A., Ramos-Cormenzana, A., 1973. Production of calcite (calcium carbonate) crystals by soil bacteria is a general phenomenon. *Nature* 246, 527–529.
- Boyd, A., Jones, S.J., 1996. Scanning electron microscopy of bone: instrument, specimen, and issues. *Microsc. Res. Tech.* 33, 92–120.
- Brown, W.E., Chow, L.C., 1981. Thermodynamics of apatite crystal-growth and dissolution. *J. Cryst. Growth* 53, 31–41.
- Brudevold, F., 1962. Chemical composition of teeth in relation to caries. In: *Sognaes, R.f. (Ed.), Chemistry and Prevention of Dental Caries*. Thomas-Springfield, pp. 32–78.
- Bryers, J.D., Ratner, B.D., 2006. Biomaterials approaches to combating oral biofilms and dental disease. *BMC Oral Health* 6, S15–S22.
- Budz, J.A., Lo Re, M., Nancollas, G.H., 1988a. The influence of high- and low-molecular-weight inhibitors on dissolution kinetics of hydroxyapatite and human enamel in lactate buffers: a constant composition study. *J. Dent. Res.* 67, 1493–1498.
- Budz, J.A., Nancollas, G.H., 1988b. The mechanism of dissolution of hydroxyapatite and carbonated apatite in acidic solutions. *J. Cryst. Growth* 91, 490–496.
- Calcinai, B., Cerrano, C., Sara, M., 2000. Borino sponges (Porifera. Demospongiae) from the Indian Ocean. *Ital. J. Zool.* 67, 203–219.
- Callis, G., Sterchi, D., 1998. Decalcification of bone: literature review and practical study of various decalcifying agents, methods, and their effects on bone histology. *J. Histotechnol.* 21, 49–58.
- Cameron, B., 1969. Paleozoic shell-boring annelids and their trace fossils. *Am. Zool.* 9, 689–703.
- Carano, A., Schlesinger, P.H., Athanasou, N.A., Teitelbaum, S.L., Blair, H.C., 1993. Acid and base effects on avian osteoclast activity. *Am. J. Physiol. Cell Physiol.* 264, C694–C701.
- Cariker, M.R., Schaadt, J.G., Peters, V., 1974. Analysis by slow-motion picture photography and scanning electron microscopy of radular function in *Urosalpinx cinerea follyensis* (Muricidae, Gastropoda) during shell penetration. *Mar. Biol.* 25, 63–76.
- Carriker, M.R., 1961. Comparative functional morphology of boring mechanisms in gastropods. *Am. Zool.* 1, 263–266.
- Carriker, M.R., 1978. Ultrastructural analysis of dissolution of shell of the bivalve *Mytilus edulis* by the accessory boring organ of the gastropod *Urosalpinx cinerea*. *Mar. Biol.* 48, 105–134.
- Carriker, M.R., Smith, E.H., 1969. Comparative calcibiocavology: summary and conclusions. *Am. Zool.* 9, 1011–1020.
- Carriker, M.R., van Zandt, D., Charlton, G., 1967. Gastropod urosalpinx: pH of accessory boring organ while boring. *Science* 158, 920–922.
- Carriker, M.R., Williams, L.G., 1978. Chemical mechanism of shell penetration by *Urosalpinx*: an hypothesis. *Malacologia* 17, 142–156.
- Chave, K.E., 1984. Physics and chemistry of biomineralization. *Ann. Rev. Earth Planet. Sci.* 12, 293–305.
- Chen, W.C., Nancollas, G.H., 1986. The kinetics of dissolution of tooth enamel. A constant composition study. *J. Dent. Res.* 65, 663–668.
- Chetal, M., Fournie, J., 1969. Shell-boring mechanism of the gastropod purpura (Thais) lapillus: a physiological demonstration of the role of carbonic anhydrase in the dissolution of  $\text{CaCO}_3$ . *Am. Zool.* 9, 983–990.
- Chockalingam, S., 1974. Nature and composition of the cephalic and thoracic cuticles of the hermit crab *Clibanarius olivaceus*. *Mar. Biol.* 26, 329–351.
- Chow, L., Markovic, C., Takagi, M.S., 2003. A dual constant-composition titration system as an *in vitro* resorption model for comparing dissolution rates of calcium phosphate biomaterials. *J. Biomed. Mater. Res. B* 65, 245–251.
- Christoffersen, J., Christoffersen, M.R., 1992. A revised theory for the growth of crystals by surface nucleation. *J. Cryst. Growth* 121, 608–616.
- Christoffersen, J., Christoffersen, M.R., 1979. Kinetics of dissolution of calcium hydroxy apatite. *J. Cryst. Growth* 47, 671–679.
- Chughtai, I., Knight-Jones, E.W., 1988. Burrowing into limestone by sabellid polychaetes. *Zool. Scr.* 17 (3), 231–238.
- Clelland, E.S., Saleuddin, A.S.M., 2000. Vacuolar-type ATPase in the accessory boring organ of *Nucella lamellosa* (Gmelin) (Mollusca: Gastropoda): role in shell penetration. *Biol. Bull.* 198, 272–283.
- Cobb, W.R., 1969. Penetration of calcium carbonate substrates by the boring sponge, *Clypea*. *Am. Zool.* 9, 783–790.
- Compere, P., Jaspars-Versali, M.-F., Goffinet, G., 2002. Glycoproteins from the Cuticle of the Atlantic Shore Crab *Carcinus maenas*. I. Electrophoresis and Western blot analysis by use of lectins. *Biol. Bull.* 202, 61–73.
- Compton, R.G., Brown, C.A., 1995. The inhibition of calcite dissolution/precipitation: 1,2-dicarboxylic acids. *J. Colloid Interf. Sci.* 170, 586–590.
- Compton, R.G., Sanders, G.H.W., 1993. The dissolution of calcite in aqueous acid: the influence of humic species. *J. Colloid Interf. Sci.* 158, 439–445.
- Crane, N.J., Popescu, V., Morris, M.D., Steenhuis, P., Ignelzi Jr., M.A., 2006. Raman spectroscopic evidence for calcium phosphate and other transient mineral species deposited during intramembranous mineralization. *Bone* 39, 343–442.
- Cui, F.Z., Li, Y., Ge, J., 2007. Self-assembly of mineralized collagen composites. *Mater. Sci. Eng. R* 57, 1–27.
- Cuif, J.-P., Dauphin, Y., Gautret, P., 1999. Compositional diversity of soluble mineralizing matrices in some recent coral skeletons compared to fine-scale growth structures of fibres: discussion of consequences for biomineralization and diagenesis. *Int. J. Earth Sci.* 88, 582–592.
- Cuif, J.-P., Dauphin, Y., 2004. The environment recording unit in coral skeletons: structural and chemical evidences of a biochemically driven stepping-growth process in coral fibres. *Biogeosci. Discuss.* 1, 625–658.
- Cvejic, J., Tambuette, S., Lotto, S., Mikov, M., Slacanin, I., Allemand, D., 2007. Determination of canthaxanthin in the red coral (*Corallium rubrum*) from Marseille by HPLC combined with UV and MS detection. *Mar. Biol.* 152, 855–862.
- Daculsi, G., LeGeros, R., Mitre, Z.D., 1989. Crystal dissolution of biological and ceramic apatites. *Calcif. Tissue Int.* 45, 95–103.
- Dalas, E., Ioannou, P.V., Koutsoukos, P.G., 1990. *In vitro* calcification: effect of molecular variables of the phospholipid molecule. *Langmuir* 6, 535–538.
- Dalas, E., Kallitsis, J.K., Koutsoukos, P.G., 1991. Crystallization of hydroxyapatite on polymers. *Langmuir* 7, 1822–1826.

- Dawes, C., 2003. What is the critical pH and why does a tooth dissolve in acid? *J. Can. Dent. Assoc.* 69, 722–724.
- Dawes, C., 2006. Why does supragingival calculus form preferentially on the lingual surface of the 6 lower anterior teeth? *J. Can. Dent. Assoc.* 70, 923–926.
- Dawes, C., Jenkins, G.N., 1962. Some inorganic constituents of dental enamel and their relationship to early calculus formation and caries. *Arch. Oral Biol.* 7, 161–172.
- de Rooij, J.F., Nancollas, G.H., 1984. The formation and remineralization of artificial white spot lesions: a constant composition approach. *J. Dent. Res.* 63, 864–867.
- Dehbi, H., Thomas, G., 1987. Thermodynamic and kinetic experimental study of the calcium phosphate dissolution in water. *Ann. Chim. (Paris, France)* 12, 47–70.
- Demadis, K.D., Neofotistou, E., Mavredaki, E., Tsiknakis, M., Sarigiannidou, E.-E., Katarachia, S.D., 2005. Inorganic foulants in membrane systems: chemical control strategies and the contribution of “green chemistry”. *Desalination* 179, 281–295.
- Demadis, K.D., Lykoudis, P., Raptis, R.G., Mezei, G., 2006. Phosphonopolycarboxylates as chemical additives for calcite scale dissolution and metallic corrosion inhibition based on a calcium-phosphonotricarboxylate organic–inorganic hybrid. *Cryst. Growth Des.* 6, 1064–1067.
- Demir, F., Dönmez, B., Çolak, S., 2003. Leaching kinetics of magnesite in citric acid solutions. *J. Chem. Eng. Jpn.* 36, 683–688.
- Dittrich, M., Obst, M., 2004. Are picoplankton responsible for calcite precipitation in lakes? *Ambio* 33, 559–563.
- Dorozhkin, S.V., 2002. A review on the dissolution models of calcium apatites. *Prog. Cryst. Growth Charact. Mater.* 44, 45–61.
- Dorozhkin, S.V., 2007. Calcium orthophosphate. *J. Mater. Sci.* 42, 1061–1095.
- Ehrlich, H.L., 1996. *Geomicrobiology*. Marcel Dekker, New York.
- Ehrlich, H., Etnoyer, P., Litvinov, S.D., Olenikova, M.M., Domaschke, H., Hanke, T., Born, R., Meissner, H., Worch, H., 2006. Biomaterial structure in deep-sea bamboo coral (Anthozoa: Scleractinia: Isididae): perspectives for the development of bone implants and templates for tissue engineering. *Mater. -Wiss. u. Werkstofftech.* 37 (6), 552–557.
- Ehrlich, H., Koutsoukos, P.G., Demadis, K.D., Pokrovsky, O.S., 2008. Principles of demineralization: modern strategies for the isolation of organic frameworks. Part I. Common definitions and history. *Micron* (doi:10.1016/j.micron.2008.02.004).
- Eggert, F.M., Germain, J.P., 1979. Rapid demineralization in acidic buffers. *Histochemistry* 59, 215–224.
- Fabritius, H., Walther, P., Ziegler, A., 2005. Architecture of the organic matrix in the sternal CaCO<sub>3</sub> deposits of *Porcellio scaber* (Crustacea: Isopoda). *J. Struct. Biol.* 150, 190–199.
- Fabritius, H., Ziegler, A., 2003. Analysis of CaCO<sub>3</sub> deposit formation and degradation during the molt cycle of the terrestrial isopod *Porcellio scaber* (Crustacea: Isopoda). *J. Struct. Biol.* 142, 281–291.
- Ferris, F.G., Wiese, R.G., Fyfe, W.S., 1994. Precipitation of carbonate minerals by microorganisms: implications for silicate weathering and the global carbon dioxide budget. *Geomicrobiol. J.* 12, 1–13.
- Ferris, F.G., Phoenix, V., Fujita, Y., Smith, R.W., 2003. Kinetics of calcite precipitation induced by ureolytic bacteria at 10 and 20 °C in artificial groundwater. *Geochim. Cosmochim. Acta* 67, 1701–1722.
- Fine, M., Tchernov, D., 2007. Scleractinian coral species survive and recover from decalcification. *Science* 315, 1811.
- Finke, M., Jandt, K.D., Parker, D.M., 2000. The early stages of native enamel dissolution studied with atomic force microscopy. *J. Colloid Interf. Sci.* 232, 156–164.
- Fosdick, L.S., Hutchinson, A.C.W., 1965. The mechanism of caries of dental enamel. *Ann. NY Acad. Sci.* 131, 758–770.
- Franc, S., Ledger, P.W., Garrone, R., 1985. Structural variability of collagen fibers in the calcareous axial rod of a sea pen. *J. Morphol.* 184, 75–84.
- Frye, G., Thomas, M., 1993. Adsorption of organic compounds on carbonate minerals. 2. Extraction of carboxylic acids from recent and ancient carbonates. *Chem. Geol.* 109, 215–226.
- Fredd, C.N., Fogler, H.S., 1998a. The influence of chelating agents on the kinetics of calcite dissolution. *J. Colloid Interf. Sci.* 204, 187–197.
- Fredd, C.N., Fogler, H.S., 1998b. The kinetics of calcite dissolution in acetic acid solutions. *Chem. Eng. Sci.* 53, 3863–3874.
- Fukuda, I., Ooki, S., Fujita, T., Murayama, E., Nagasawa, H., Isa, Y., Watanabe, T., 2003. Molecular cloning of a cDNA encoding a soluble protein in the coral exoskeleton. *Biochem. Biophys. Res. Commun.* 304, 11–17.
- Fujita, Y., Ferris, F.G., Lawson, R.D., Colwell, F.S., Smith, R.W., 2000. Calcium carbonate precipitation by ureolytic subsurface bacteria. *Geomicrobiol. J.* 17, 305–318.
- Garcia-Pichel, F., 2006. Plausible mechanisms for the boring on carbonates by microbial phototrophs. *Sedim. Geol.* 185, 205–213.
- Gerstenfeld, L.C., Feng, M., Gotoh, Y., Glimcher, M.J., 1994. Selective extractability of noncollagenous proteins from chicken bone. *Calcif. Tissue Int.* 55, 230–235.
- Glimcher, M.J., Katz, E.P., Travis, D.F., 1965. The solubilization and reconstruction of bone collagen. *J. Ultrastruct. Res.* 13, 163–171.
- Glimcher, M.J., 2006. Bone: nature of the calcium phosphate crystals and cellular, structural, and physical chemical mechanisms in their formation. *Rev. Mineral. Geochem.* 64, 223–282.
- Golubev, S.V., Bauer, A., Pokrovsky, O.S., 2006. Effect of pH and organic ligands on the kinetics of smectite dissolution at 25 °C. *Geochim. Cosmochim. Acta* 70, 4436–4451.
- Golubev, S.V., Pokrovsky, O.S., 2006. Experimental study of the effect of organic ligands on diopside dissolution kinetics. *Chem. Geol.* 235, 377–389.
- Golubev, S.V., Pokrovsky, O.S., Oelkers, E.H., Benzeith, P., submitted for publication. Role of organic ligands in calcite dissolution at 25 °C. *Geochim. Cosmochim. Acta*.
- Golubic, S., Campbell, S.E., Drobne, K., Cameron, B., Blasman, W.L., Cimmermann, F., Dubois, L., 1984. Microbial endoliths: a benthic overprint in the sedimentary record, and a paleobathymetric cross-reference with foraminifera. *J. Paleontol.* 58, 351–361.
- Gotoh, Y., Gerstenfeld, L.G., Glimcher, M.J., 1990. Identification and characterization of the major chicken bone phosphoprotein. Analysis of its synthesis by cultured embryonic chick osteoblasts. *Eur. J. Biochem.* 187, 49–58.
- Gotoh, Y., Salih, E., Glimcher, M.J., Gerstenfeld, L.C., 1995. Characterization of the major non-collagenous proteins of chicken bone: identification of a novel 60 kDa non-collagenous phosphoprotein. *Biochem. Biophys. Res. Commun.* 208, 863–870.
- Graf, F., 1967. Dynamique du calcium dans l'épithélium des caecums postérieurs d'*Orchestia cavimana* Heller (Crustacea: Amphipode): rôle de l'espace intercellulaire. *C. R. Acad. Sci. Paris* 273, 1828–1831.
- Gramain, P., Thomann, J.M., Gumpfer, M., Voegel, J.C., 1989. Dissolution kinetics of human enamel powder. I. Stirring effects and surface calcium accumulation. *J. Colloid Interf. Sci.* 128, 370–381.
- Grynaps, M.D., Omelon, S., 2007. Transient precursor strategy or very small biological apatite crystals? *Bone* 41 (2), 162–164.
- Gustafson, G.T., Lerner, U., 1984. Bradykinin stimulates bone resorption and lysosomal-enzyme release in cultured mouse calvaria. *Biochem. J.* 219, 329–332.
- Habelitz, S., Balooch, M., Marshall, S.J., Balooch, G., Marshall Jr., G.W., 2002. In situ atomic force microscopy of partially demineralized human dentin collagen fibrils. *J. Struct. Biol.* 138, 227–236.
- Haigler, S.A., 1969. Boring mechanism of *Polydora websteri* inhabiting *Crassostrea virginica*. *Am. Zool.* 9, 821–828.
- Hamdona, S.K., Hamza, S.M., Mangood, A.H., 1995. Effect of some amino acids on the rate of dissolution of calcite crystals in aqueous systems. *Desalination* 101, 263–267.
- Hannig, C., Hamkens, A., Becker, K., Attin, R., Attin, T., 2005. Erosive effects of different acids on bovine enamel: release of calcium and phosphate *in vitro*. *Arch. Oral Biol.* 50, 541–552.
- Harper, E.M., 2005. Evidence of predation damage in Pliocene *Apletosia maxima* (Brachiopoda). *Palaeontology* 48, 1–12.
- Hassenkam, T., Fanther, G.E., Cutroni, J.A., Weaver, J.C., Morse, D.E., Hansma, P.K., 2004. High-resolution AFM imaging of intact and fractured trabecular bone. *Bone* 35, 4–10.
- Hatch, W.L., 1980. The implication of carbonic anhydrase in the physiological mechanism of penetration of carbonate substrata by the marine burrowing sponge *Cliona celata* (Demospongiae). *Biol. Bull.* 159, 135–147.
- Hayashi, Y., Yanagiguchi, K., Virolia, I., Yukizaki, H., 1997. High-resolution electron microscopy of crystal contact in the demineralized dentine. *J. Electron. Microsc.* 46, 189–192.
- Hayward, D.C., Samuel, P.C., Pontynen, Catmull, J., Saint, R., Miller, D.J., Ball, E.E., 2002. *Proc. Natl. Acad. Sci. U.S.A.* 99, 8111–8116.
- Hecker, A., Quenedey, B., Testaniere, O., Quenedey, A., Graf, F., Luquet, G., 2004. Orchestrin, a calcium-binding phosphoprotein, is a matrix component of two successive transitory calcified biomineralizations cyclically elaborated by a terrestrial crustacean. *J. Struct. Biol.* 146, 310–324.
- Hecker, A., Testaniere, O., Marin, F., Luquet, G., 2003. Phosphorylation of serine residues is fundamental for the calcium-binding ability of Orchestrin, a soluble matrix protein from crustacean calcium storage structures. *FEBS Lett.* 535, 49–54.
- Hoch, A.R., Reddy, M.M., Aiken, G.R., 2000. Calcite crystal growth inhibition by humic substances with emphasis on hydrophobic acids from the Florida Everglades. *Geochim. Cosmochim. Acta* 64, 61–72.
- Inoue, M., Yoshida, H., Akisaka, T., 1999. Visualization of acidic compartments in cultured osteoclasts by use of an acidotropic amine as a marker for low pH. *Cell Tissue Res.* 298, 527–537.
- Ishii, K., Tsutsui, N., Watanabe, T., Yanagisawa, T., Nagasawa, H., 1998. Solubilization and chemical characterization of an insoluble matrix protein in the gastroliths of a crayfish, *Procambarus clarkii*. *Biosci. Biotechnol. Biochem.* 62, 291–296.
- Ishii, K., Yanagisawa, T., Nagasawa, H., 1996. Characterization of a matrix protein in the gastroliths of the crayfish *Procambarus clarkii*. *Biosci. Biotechnol. Biochem.* 60, 1479–1482.
- Isik, G., Ince, S., Saglam, F., Onan, U., 1997. Comparative SEM study on the effect of different demineralization methods with tetracycline HCl on healthy root surfaces. *J. Clin. Periodontol.* 24, 589–594.
- Jackson, D.J., Macis, L., Reitner, J., Degnan, B.M., Wörheide, G., 2007. Sponge paleogenomics reveals an ancient role for carbonic anhydrase in skeletogenesis. *Science* 316, 1893–1895.
- Jenkins, J.N., 1978. *The Physiology and Biochemistry of the Mouth*, 4th ed. Blackwell Science, 599 pp.
- Johnston, I.S., 1980. The ultrastructure of skeletogenesis in hermatypic corals. *Int. Rev. Cytol.* 67, 171–214.
- Jordan, G., Pokrovsky, O.S., Guichet, X., Schmall, W., 2007. Organic and inorganic ligand effects on magnesite dissolution at 100 °C and pH 5–10. *Chem. Geol.* 242, 484–496.
- Jung, W.J., Jo, G.H., Kuk, J.H., Kim, Y.J., Oh, K.T., Park, R.D., 2007. Production of chitin from red crab shell waste by successive fermentation with *Lactobacillus paracasei* KCTC-3074 and *Serratia marcescens* FS-3. *Carbohydr. Polym.* 68, 746–750.
- Jung, W.J., Kuk, J.H., Kim, K.Y., Park, R.D., 2005. Demineralization of red crab shell waste by lactic acid fermentation. *Appl. Microbiol. Biotechnol.* 67, 851–854.

- Kalinowski, B.E., Liermann, L.J., Brantley, S.L., Barnes, A., Pantano, C.G., 2000. X-ray photoelectron evidence for bacteria-enhanced dissolution of hornblende. *Geochim. Cosmochim. Acta* 64, 1331–1343.
- Kibby, C.L., Hall, W.K., 1972. Surface properties of calcium phosphates. In: Hair, M.L. (Ed.), *The Chemistry of Biosurface II*. Marcel Dekker, NY, pp. 663–729.
- Kingsley, R.J., Tsuzaki, M., Watabe, N., Mechanic, G.L., 1995. Collagen in the spicule organic matrix of the gorgonian *leptogorgia virgulata*. *Biol. Bull.* 79, 203–213.
- Kitano, Y., 1962. Polymorphic formation of calcium carbonate in thermal springs with an emphasis on the effect of temperature. *Bull. Chem. Soc. Jpn.* 35, 1980–1985.
- Kossel, W., 1934. Zur energetik fur oberflächenvorgängen. *Ann. Phys.* 21, 457–480.
- Koutsoukos, P.G., 1998. Influence of metal ions on the crystal growth of calcium phosphates. In: Amjad, Z. (Ed.), *Calcium Phosphates in Biological and Industrial Systems*. Kluwer Academic Publishers, pp. 145–171.
- Koutsoukos, P.G., Valsami-Jones, E., 2003. Phosphorus removal technologies from water and wastewater. In: Valsami-Jones, E. (Ed.), *Phosphorus in Environmental Technology: Principles and Applications*. IWA Publishing, London, pp. 193–248.
- Kreitzman, S.N., Fritz, M.E., 1970. Demineralization of bone by phosphoprotein phosphatase. *J. Dent. Res.* 49, 1509–1512.
- Kreitzman, S.N., Fritz, M.E., Saffir, A.J., 1970. Enzymatic destruction of bone *in vitro*. *Nature* 228, 575–576.
- Kreitzman, S.N., Irving, S., Navia, J.M., Harris, R.S., 1969. Enzymatic release of phosphate from rat molar enamel by phosphoprotein phosphatase. *Nature* 223, 520–521.
- Laçin, O., Dönmez, B., Demir, F., 2005. Dissolution kinetics of natural magnesite in acetic acid solutions. *Int. J. Miner. Process.* 75, 91–99.
- Lafon, M., 1948. Nouvelles recherches biochimiques et physiologiques sur le squelette tegumentaire des crustacés. *Bull. Inst. Oceanogr.* 45, 1–28.
- Lazar, B., 1991. Bioerosion of coral reefs—a chemical approach. *Limnol. Oceanogr.* 36, 377–383.
- Lewandrowski, K.-U., Tomford, W.W., Michaud, N.A., Schomaker, K.T., Deutsch, T.F., 1997. An electron microscopic study on the process of acid demineralization of cortical bone. *Calcif. Tissue Int.* 61, 294–297.
- Lewandrowski, K.U., Venugopalan, V., Tomford, W.W., Schomacker, K.T., Mankin, H.J., Deutsch, T.F., 1996. Kinetics of cortical bone demineralisation. A new method for modifying cortical bone allografts. *J. Biomat. Res.* 31, 365–372.
- Lian, B., Hu, Q., Chen, J., Ji, J., Teng, H.H., 2006. Carbonate biomineralization induced by soil bacterium *Bacillus megaterium*. *Geochim. Cosmochim. Acta* 70, 5522–5535.
- Lijun, T.R., Bonstein, T., Orme, C.A., Bush, P.J., Nancollas, G.H., 2005. A new model for nanoscale enamel dissolution. *J. Phys. Chem. B* 109, 999–1005.
- Lindskog, S., 1997. *Pharmacol. Ther.* 74, 1–20.
- Lippert, F., Parker, D.M., Jandt, K.D., 2004. *In vitro* demineralization/remineralization cycles at human tooth enamel surfaces investigated by AFM and nanoindentation. *J. Colloid Interf. Sci.* 280, 442–448.
- Liu, P.-J., Hsieh, H.-L., 2000. Burrow architecture of the spionid polychaete *Polydora villosa* in the corals *Montipora* and *Porites*. *Zool. Stud.* 39 (1), 47–54.
- Löwenstam, H.A., 1971. Phosphatic hard tissues of marine invertebrates: their nature and mechanical function and some fossil implications. *Chem. Geol.* 9, 153–166.
- Lower, S.K., Maurice, P.A., Traina, S.J., 1998. Simultaneous dissolution of hydroxylapatite and precipitation of hydroxypyromorphite: direct evidence of homogeneous nucleation. *Geochim. Cosmochim. Acta* 62, 1773–1780.
- Lucas, J.M., Knapp, L.W., 1996. Biochemical characterization of purified carbonic anhydrase from the octocoral *Leptogorgia virgulata*. *Mar. Biol.* 126, 471–477.
- Ludwig, C., Casey, W.H., Rock, P.A., 1995. Prediction of ligand-promoted dissolution rates from the reactivities of aqueous complexes. *Nature* 375, 44–47.
- Lunz, G.R., 1940. The annelid worm, *Polydora*, as an oyster pest. *Science* 92, 310.
- Luquet, G., Marin, F., 2004. Biomineralisations in crustaceans: storage strategies. *C. R. Palevol.* 3, 515–534.
- Margolis, H.C., Moreno, E.C., 1992. Kinetics of hydroxyapatite dissolution in acetic, lactic and phosphoric acid solutions. *Calcif. Tissue Int.* 50, 137–143.
- Marin, F., Luquet, G., 2007. Unusually acidic proteins in biomineralization. In: Bäuerlein, E. (Ed.), *Handbook of Biomineralization*. Wiley-VCH, Weinheim, pp. 273–290.
- Marshall Jr., G.W., Balooch, M., Tench, R.J., Kinney, J.H., Marshall, S.J., 1993. Atomic force microscopy of acid effects on dentin. *Dent. Mater.* 9, 265–268.
- Martin, D., Britayev, T.A., 1998. Symbiotic polychaetes: review of known species. *Oceanogr. Mar. Biol. Ann. Rev.* 36, 217–340.
- Mayer, I., Voegel, J.C., Bres, E.F., Frank, R.M., 1988. The release of carbonate during the dissolution of synthetic apatites and dental enamel. *J. Cryst. Growth* 87, 129–136.
- McDowell, H., Gregory, T.M., Brown, W.E., 1977. Solubility of hydroxyapatite ( $\text{Ca}_5(\text{PO}_4)_3\text{OH}$ ) in the system calcium hydroxide-phosphoric acid-water at 5, 15, 25, and 37 °C. *J. Res. Natl. Bureau Stand. A: Phys. Chem.* 81A, 273–281.
- Melikhov, I.V., Doroshkin, S.V., Nikolaev, A.L., Kozlovskaya, E.D., Rudin, V.N., 1990. Dislocations and dissolution rates of solids. *Z. Fiz. Khim.* 64, 3242–3248.
- Meyran, J.C., Graf, F., Fournie, J., 1987. Carbonic anhydrase activity in a calcium-mobilizing epithelium of the crustacean *Orchestia cavimana* during molting. *Histochemistry* 87, 419–429.
- Miles, A.E.W., 1967. *Structural and Chemical Organization of the Teeth*. Academic Press, London, 525 pp.
- Mitchell, A.C., Ferris, F.G., 2006. The influence of *Bacillus pasteurii* on the nucleation and growth of calcium carbonate. *Geomicrobiol. J.* 23, 213–226.
- Moreno, E.C., Zahradnik, R.T., 1974. Chemistry of enamel subsurface demineralization *in vitro*. *J. Dent. Res.* 53, 226–235.
- Monger, H.C., Daugherty, L.A., Lindemann, W.C., Liddell, C.M., 1991. Microbial precipitation of pedogenic calcite. *Geology* 19, 997–1000.
- Morita, R.Y., 1980. Calcite precipitation by marine bacteria. *Geomicrobiol. J.* 2, 63–82.
- Morton, B., Scott, P.J.B., 1988. Evidence for chemical boring in *Petricola lapicida* (Gmelin 1791) (Bivalvia: Petricoliidae). *J. Moll. Stud.* 54, 231–237.
- Mullin, J.W., 1993a. *Crystallization*, 3rd ed. Butterworth-Heinemann, London, 570 pp.
- Mullin, J.W., 1993b. *Crystallization*, 3rd ed. Butterworth-Heinemann, Oxford.
- Nancollas, G.H., 1966. *Intractions in Electrolyte Solutions*. Elsevier, Amsterdam/London/New York, 214 pp.
- Nancollas, G.H., 1989. *In vitro* studies of calcium phosphate crystallization. In: Mann, S., Webb, J., Williams, R.J.P. (Eds.), *Biomineralization*. VCH, Basel, pp. 156–187.
- Nancollas, G.H., Wu, W., 2000. Biomineralization mechanisms: a kinetics and interfacial energy approach. *J. Cryst. Growth* 211 (1–4), 137–142.
- Nancollas, G.H., 1992. The involvement of calcium phosphates in biological mineralization and demineralization processes. *Pure Appl. Chem.* 64 (11), 1673–1678.
- Nancollas, W.F., Bareham, B.J., 1975. Evidence for the presence of secondary calcium phosphate in bone and its stabilization by acid production. *Calcif. Tissue Res.* 18, 161–172.
- Noé, S.U., Dullo, W.-C., 2006. Skeletal morphogenesis and growth mode of modern and fossil deep-water isidid gorgonians (Octocorallia) in the West Pacific (New Zealand and Sea of Okhotsk). *Coral Reefs* 25, 303–320.
- Nordström, T., Shrode, L.D., Rotstein, O.D., Romanek, R., Goto, T., Heersche, J.N.M., Manolón, M.F., Brisseau, G.F., Grinstein, S., 1997. Chronic extracellular acidosis induces plasmalemmal vacuolar type  $\text{H}^+\text{ATPase}$  activity in osteoclasts. *J. Biol. Chem.* 272, 6354–6360.
- Oliveira, S.S.A., Marshall, S.J., Hilton, J.F., Marshall, G.W., 2002. Etching kinetics of a self-etching primer. *Biomaterials* 23, 4105–4112.
- Oltsza, M.J., Cheng, X., Jee, S.S., Kumar, R., Kim, Y.Y., Kaufman, M.J., Douglas, E.P., Gower, L.B., 2007. Bone structure and formation: a new perspective. *Mater. Sci. Eng. R* 58, 77–116.
- Parolo, C.C.F., Maltz, M., 2006. Microbial contamination of noncavitated caries lesions: a scanning electron microscopic study. *Caries Res.* 40, 536–541.
- Paschalis, E.P., Tan, J., Nancollas, G.H., 1996. Constant composition dissolution kinetics studies of human dentin. *J. Dent. Res.* 75, 1019–1026.
- Patel, P.R., Brown, W.E., 1975. Thermodynamic solubility product of human tooth enamel. *J. Dent. Res.* 54, 728–736.
- Patel, M.V., Fox, J.L., Higuchi, W.I., 1987. Effect of acid type on kinetics and mechanism of dental enamel demineralization. *J. Dent. Res.* 66, 1425–1430.
- Pawlowski, J., Holzmann, M., Berney, C., Fahrni, J., Gooday, A.J., Cedhagen, T., Habura, A., Bowser, S., 2003. The evolution of early Foraminifera. *Proc. Natl. Acad. Sci. U.S.A.* 100, 11494–11498.
- Peterson, L.G., 1975. On topical Application of Fluorides and its Inhibiting Effect on Caries. Thesis. University of Lund. *Odont. Rev.* 26 suppl. 34.
- Perrin, C., 2003. Compositional heterogeneity and microstructural diversity of coral skeletons: implications for taxonomy and control on early diagenesis. *Coral Reefs* 22, 109–120.
- Perry, T.D., Duckworth, I.V., McNamara, O.W., Martin, C.J., Mitchell, S.T.R., 2004. Effects of the biologically produced polymer alginate on microscopic calcite dissolution rates. *Environ. Sci. Technol.* 38, 3040–3046.
- Perry, T.D., Duckworth, O.W., Kendall, T.A., Martin, S.T., Mitchell, R., 2005. Chelating ligand alters the microscopic mechanism of mineral dissolution. *J. Am. Chem. Soc.* 127, 5744–5745.
- Pokrovsky, O.S., Savenko, V.S., 1994. Influence of dissolved organic matter on the kinetics of homogeneous precipitation of aragonite in seawater. *Oceanology* 34, 760–767.
- Pokrovsky, O.S., Savenko, V.S., 1995. Experimental modeling of  $\text{CaCO}_3$  precipitation at the conditions of photosynthesis in seawater. *Oceanology* 35, 805–810.
- Pokrovsky, O.S., Schott, J., 2001. Kinetics and mechanism of dolomite dissolution in neutral to alkaline solutions revisited. *Am. J. Sci.* 301, 597–626.
- Pokrovsky, O.S., Schott, J., Castillo, A., 2005. Kinetics of brucite dissolution at 25 °C in the presence of organic and inorganic ligands and divalent metals. *Geochim. Cosmochim. Acta* 69, 905–918.
- Pokrovsky, O.S., Golubev, S.V., Jordan, G., 2008. Effect of organic and inorganic ligands on calcite and magnesite dissolution rates at 60 °C and 30 atm  $\text{pCO}_2$ . *Chem. Geol.* (in review).
- Pomponi, S.A., 1980. Cytological mechanisms of calcium carbonate excavation by boring sponges. *Int. Rev. Cytol.* 65, 301–319.
- Plummer, L.N., Busenberg, E., 1982. The solubilities of calcite, aragonite and vaterite in  $\text{CO}_2$ - $\text{H}_2\text{O}$  solutions between 0 and 90 °C. *Geochim. Cosmochim. Acta* 46, 1011–1040.
- Puverel, S., Tambuette, E., Zoccola, D., Domart-Coulon, I., Bouchot, A., Lotto, S., Allemand, D., Tambuette, S., 2005a. Antibodies against the organic matrix in scleractinians: a new tool to study coral biomineralization. *Coral Reefs* 24, 149–156.
- Puverel, S., Tambuette, E., Pereira-Mouries, L., Zoccola, D., Allemand, D., Tambuette, S., 2005b. Soluble organic matrix of two Scleractinian corals: partial and comparative analysis. *Comp. Biochem. Physiol. Part B* 141, 480–487.
- Raabe, D., Romano, P., Sachs, C., Al-Sawalmih, A., Brokmeier, H.-G., Yi, S.-B., Servos, G., Hartwig, H.G., 2005a. Discovery of a honeycomb structure in the twisted plywood patterns of fibrous biological nanocomposite tissue. *J. Cryst. Growth* 283, 1–7.

- Raabe, D., Romano, P., Sachs, C., Fabritius, H., Al-Sawalmih, A., Yi, S.-B., Servos, G., Hartwig, H.G., 2006. Microstructure and crystallographic texture of the chitin-protein network in the biological composite material of the exoskeleton of the lobster *Homarus americanus*. *Mater. Sci. Eng. A* 421, 143–153.
- Raabe, D., Sachs, C., Romano, P., 2005b. The crustacean exoskeleton as an example of a structurally and mechanically graded biological nanocomposite material. *Acta Mater.* 53, 4281–4292.
- Rahman, M.A., Isa, Y., 2005. Characterization of proteins from the matrix of spicules from the alcyonarian, *Lobophytum crassum*. *J. Exp. Mar. Biol. Ecol.* 321, 71–82.
- Raz, S., Testeniere, O., Hecker, A., Weiner, S., Luquet, G., 2002. Stable amorphous calcium carbonate is the main component of the calcium storage structures of the crustaceans *Orchestria cavimana*. *Biol. Bull.* 203, 269–274.
- Risk, J.M., Samarco, W.P., Dinger, N.E., 1995. Bioerosion in *Acropora* across the continental shelf of the Great Barrier Reef. *Coral Reefs* 14, 79–86.
- Robinson, C., Shore, R.C., Brookes, S.J., Strafford, S., Wood, S.R., Kirkham, J., 2000. The chemistry of enamel caries. *Crit. Rev. Oral Biol. Med.* 11 (4), 481–495.
- Rodríguez-Navarro, C., Jiménez-Lopez, C., Rodríguez-Navarro, A., González-Muñoz, M.T., Rodríguez-Gallego, M., 2007. Bacterially mediated mineralization of vaterite. *Geochim. Cosmochim. Acta* 71, 1197–1213.
- Roer, R., Dillaman, R., 1984. The structure and calcification of the crustacean cuticle. *Am. Zool.* 24, 893–909.
- Romano, P., Fabritius, H., Raabe, D., 2007. The exoskeleton of the lobster *Homarus americanus* a san example of a smart anisotropic biological material. *Acta Biomater.* 3, 301–309.
- Rützler, K., Rieger, G., 1973. *Mar. Biol.* 21, 144–162; Rützler, K., 1975. *Oecologia (Berlin)* 19, 203–216.
- Sachs, C., Fabritius, H., Raabe, D., 2006. Hardness and elastic properties of dehydrated cuticle from the lobster *Homarus americanus* obtained by nanoindentation. *J. Mater. Res.* 21, 1987–1995.
- Schiemenz, P., 1891. Wie bohrt *Natica* die Muscheln an? *Mitt. Zool. Sta. Neapel.* 10, 153–169.
- Schmidt-Nielsen, B., 1946. The solubility of tooth substance in relation to the composition of saliva. *Acta Odontol. Scand.* 7 (Suppl. 2), 1–88.
- Schönberg, C.H.L., 2002a. *Pione lampa*, a bioeroding sponge in a worm reef. *Hydrobiologia* 482, 49–68.
- Schönberg, C.H.L., 2002b. Substrate effects on the bioeroding demosponge *Cliona orientalis*. 1. Bioerosion rates. *Mar. Ecol. Prog. Ser.* 233, 313–326.
- Schönberg, C.H.L., 2006. Growth and erosion of the zooxanthellate Australian bioeroding sponge *Cliona orientalis* are enhanced in light. In: *Proceedings of the 10th International Coral Reef Symposium*, pp. 168–174.
- Schüpbach, P., Guggenheim, B., Lutz, F., 1989. Human root caries: histopathology of initial lesions in cementum and dentin. *J. Oral Pathol. Med.* 18, 146–156.
- Senn, N., 1889. On the healing of aseptic bone cavities by implantation of antiseptic decalcified bone. *Am. J. Med. Sci.* 218–243.
- Schindler, P.W., Stumm, W., 1987. The surface chemistry of oxides, hydroxides, and oxide minerals. In: Stumm, W. (Ed.), *Aquatic Surface Chemistry*. Wiley, pp. 337–365.
- Scott, J.E., Kyffin, T.W., 1978. Demineralization in organic solvents by alkylammonium salts of Ethylenediamine tetra-acetic acid. *Biochem. J.* 169, 697–701.
- Sherwood, O.A., Scott, D.B., Risk, M.J., 2006. Late Holocene radiocarbon and aspartic acid racemization dating of deep-sea octocorals. *Geochim. Cosmochim. Acta* 70, 2806–2814.
- Shyu, L.J., Perez, L., Zawacki, S., Heughebaert, J.C., Nancollas, G.H., 1983. The solubility of octacalcium phosphate at 37 °C in the system calcium hydroxide-phosphoric acid-potassium nitrate-water. *J. Dent. Res.* 62, 398–400.
- Simon, P., Lichte, H., Formanek, P., Lehmann, M., Huhle, R., Carrillo-Cabrera, W., Harscher, A., Ehrlich, H., 2008. Electron holography of biological samples. *Micron* 39, 229–256.
- Sjöberg, E.L., Rickard, D.T., 1983. The influence of experimental design on the rate of calcite dissolution. *Geochim. Cosmochim. Acta* 47, 2281–2285.
- Smith, E.H., 1969. Functional morphology of *Penitella conradi* relative to shell-penetration. *Am. Zool.* 9, 869–880.
- Spanos, N., Misirlis, D.Y., Kanellou, D.G., Koutsoukos, P.G., 2006a. Seeded growth of hydroxyapatite in simulated body fluid. *J. Mater. Sci.* 41 (6), 1805–1812.
- Spanos, N., Kanellou, D.G., Koutsoukos, P.G., 2006b. The interaction of diphosphonates with calcitic surfaces: understanding the inhibition activity in marble dissolution. *Langmuir* 22, 2074–2081.
- Stanley Jr., G.D., 2003. The evolution of modern corals and their early history. *Earth-Sci. Rev.* 60, 195–225.
- Stephan, R.M., 1940. Changes in hydrogen-ion concentration on tooth surfaces and in carious lesions. *J. Am. Dent. Assoc.* 27, 718–723.
- Stevenson, J.R., 1985. Dynamics of the integument. In: Bliss, D.R., Mantel, L.H. (Eds.), *The Biology of Crustacea*. Academic Press, New York.
- Stumm, W., 1992. *Chemistry of the Solid-Water Interface*. Wiley.
- Stumm, W., Morgan, J.J., 1996. *Aquatic Chemistry*. John Wiley and Sons, New York, 792 pp.
- Takagi, Y., Ishii, K., Ozaki, N., 2000. Immunolocalization of gastrolith matrix protein (GAMP) in the gastroliths and exoskeleton of *Procambarus clarkii*. *Zool. Sci.* 17, 179–184.
- Tambutté, S., Tambutté, É., Zoccola, D., Allemand, D., 2007. Organic matrix and biomineralization of scleractinian corals. In: Baeuerlein, E. (Ed.), *Handbook of Biomineralization*, vol. 1. Wiley-VCH Verlag GmbH & Co., Weinheim, pp. 243–259.
- Tang, R., Nancollas, G.H., Orme, C.A., 2001. Mechanism of dissolution of sparingly soluble electrolytes. *J. Am. Chem. Soc.* 123, 5437–5443.
- Tang, R., Hass, M., Wu, W., Gulde, S., Nancollas, G.H., 2003. Constant composition dissolution of mixed phases. II. Selective dissolution of calcium phosphates. *J. Colloid Interf. Sci.* 26, 379–384.
- Tang, R., Nancollas, G.H., 2002. New mechanism for the dissolution of sparingly soluble minerals. *Pure Appl. Chem.* 74, 1851–1857.
- Tang, R., Wang, L., Nancollas, G., 2004a. Size-effects in the dissolution of hydroxyapatite: an understanding of biological demineralization. *J. Mater. Chem.* 14, 2341–2346.
- Tang, R., Wang, L., Orme, C.A., Bonstein, T., Bush, P.J., Nancollas, G.H., 2004b. Dissolution at the nanoscale: self-preservation of biominerals. *Angew. Chem. Int. Ed.* 43, 2697–2701.
- Tauchmanova, L., Pivonello, R., Di Somma, C., Rossi, R., De Martino, M.C., Camera, L., Klain, M., Salvatore, M., Lombardi, G., Colao, A., 2006. Bone demineralization and vertebral fractures in endogenous cortisol excess: role of disease etiology and gonadal status. *J. Clin. Endocrinol. Metab.* 91, 1779–1784.
- Ten Cate, R., 1979. Remineralization of Enamel Lesions. Ph.D. Thesis. University of Groningen, 127 pp.
- Thomas, M., Clouse, J., Longo, J., 1993. Adsorption of organic compounds on carbonate minerals. 3. Influence on dissolution rates. *Chem. Geol.* 109, 227–237.
- Thylstrup, A., Bruun, C., Holmen, L., 1994. *In vivo* caries models—mechanisms for caries initiation and arrestment. *Adv. Dent. Res.* 8, 144–157.
- Tomazic, B.B., Brown, W.E., Schoen, F.J., 1994. Physicochemical properties of calcific deposits isolated from porcine bioprosthetic heart valves removed from patients following 2–13 years function. *J. Biomater. Res.* 28, 35–47.
- Torreccilla, I., Leganes, F., Bonilla, I., Fernandez-Pinas, F., 2001. Calcium transients in response to salinity and osmotic stress in the nitrogen-fixing cyanobacterium *Anabaena* sp. PCC7120, expressing cytosolic aquaporin. *Plant Cell Environ.* 24, 641–648.
- Trautz, O.R., 1967. Crystalline organization of dental mineral. In: Miles, A.E.W. (Ed.), *Structural and Chemical Organization of Teeth*. Acad. Press, Washington, DC, pp. 165–197.
- Troschel, F.H., 1854. Über die Speichel von *Dolium galea*. *J. Prakt. Chem.* 63, 170–179.
- Vacelet, J., 1981. Algal-sponge symbiosis in the coral reefs of New Caledonia: a morphological study. In: Gomez, E.D., et al. (Eds.), *The Reef and Man. Proceedings of the 4th International Coral Reef Symp*, Manila 2, University of the Philippines, Quezon City, Philippines, pp. 713–719.
- Valsami-Jones, E., Ragnarsdottir, K.V., Putnis, A., Bosbach, D., Kemp, A.J., Cressey, G., 1998. The dissolution of apatite in the presence of aqueous metal cations at pH 2–7. *Chem. Geol.* 151, 215–233.
- Veis, A., Sabsay, B., 1983. Bone and tooth formation. Insights into mineralization strategies. In: Westbroek, P., de Jong, E.W. (Eds.), *Biomineralization and Biological Metal Accumulation*. Reidel Publishing Corporation, pp. 273–284.
- Venec-Peyre, M.-T., 1987. Boring Foraminifera in French Polynesian coral reefs. *Coral Reefs* 5, 205–212.
- Venec-Peyre, M.-T., 1996. Bioeroding foraminifera: a review. *Mar. Micropaleontol.* 28, 19–30.
- Wainwright, S.A., 1963. Skeletal organization in the coral. *Pocillopora damicornis*. *Quart. J. Micr. Sci.* 104, 169–183.
- Wang, J., Zhou, H.-Y., Salih, E., Xu, L., Wunderlich, L., Gu, X., Hofstaetter, J.G., Torres, M., Glimcher, M.J., 2006a. Site-specific *In vivo* calcification and osteogenesis simulated by bone sialoprotein. *Calcif. Tissue Int.* 79, 179–189.
- Wang, L.J., Tang, R., Bonstein, T., Bush, P., Nancollas, G.H., 2006b. Enamel demineralization in primary and permanent teeth. *J. Dent. Res.* 85, 359–363.
- Wang, L., Tang, R., Bonstein, T., Orme, C.A., Bush, P.J., Nancollas, G.H., 2005. A new model for nanoscale enamel dissolution. *J. Phys. Chem.* 109, 999–1005.
- Wang, L.J., Tang, R., Bonstein, T., Bush, P., Nancollas, G.H., 2006c. Enamel demineralization in primary and permanent teeth. *J. Dent. Res.* 85 (4), 359–363.
- Warren, L.A., Maurice, P.A., Parmar, N., Ferris, F.G., 2001. Microbially mediated calcium carbonate precipitation: implications for interpreting calcite precipitation and for solid phase capture of inorganic contaminants. *Geomicrobiol. J.* 18, 93–115.
- Watabe, N., Pan, C.-M., 1984. Phosphatic shell formation in atremate brachiopods. *Am. Zool.* 24, 977–985.
- Weatherell, J., Robinson, C., 1973. The inorganic composition of teeth. In: Zipkin, I. (Ed.), *Biological Mineralization*. Wiley, New York, pp. 43–74.
- Weiner, S., 1984. Organization of organic matrix components in mineralized tissues. *Am. Zool.* 24, 945–951.
- Weiner, S., 2006. Transient precursor strategy in mineral formation of bone. *Bone* 39, 431–433.
- Welsh, S., Vandevivere, A.P., 1994. Effect of microbial and other naturally occurring polymers on mineral dissolution. *Geomicrobiol. J.* 12, 227–238.
- Wheatly, M.G., 1999. Calcium homeostasis in crustaceans: the evolving role of branchial, renal, digestive and hypodermal epithelia. *J. Exp. Zool.* 283, 620–640.
- Wheatly, M.G., Ayers, J., 1995. Scaling of calcium, inorganic contents, and organic contents to body mass during the moulting cycle of the fresh-water crayfish *Procambarus clarkii* (Girard). *J. Crustacean Biol.* 15, 409–417.
- Williams, J.A., Margolis, S.V., 1974. Sipunculid burrows in coral reef: evidence for chemical and mechanical excavation. *Pacif. Sci.* 28, 357–359.
- Wisshak, M., Rüggeberg, A., 2006. Colonisation and bioerosion of experimental substrates by benthic foraminifera from euphotic to aphotic depths (Kosterfjord, SW Sweden). *Facies* 52, 1–17.
- Wu, Y.-T., Grant, C., 2002. Effect of chelation chemistry of sodium polyaspartate on the dissolution of calcite. *Langmuir* 18, 6813–6820.

- Yamada, T., 2004. Bone-demineralized bone–bone graft for ligament reconstruction in rats. *J. Med. Dent. Sci.* 51, 45–52.
- Yanasigawa, T., Miate, Y., 2003. High-resolution electron microscopy of enamel-crystal demineralization and remineralization in carious lesions. *J. Electron Microsc.* 52, 605–613.
- Yoshida, Y., Van Meerbeek, B., Nakayama, Y., Yoshioka, M., Snauwaert, J., Abe, Y., Lambrechts, P., Vanherle, G., Okazaki, M., 2001. Adhesion to and decalcification of hydroxyapatite by carboxylic acids. *J. Dental Res.* 80, 1565–1569.
- Yoshioka, M., Yoshida, Y., Inoue, S., Lambrechts, P., Vanherle, G., Nomura, Y., Okazaki, M., Shintani, H., Van Meerbeek, B., 2002. Adhesion/decalcification mechanisms of acid interaction with human hard tissues. *J. Biomed. Mater. Res.* 59, 56–62.
- Young, R.A., 1975. Biological apatite vs. hydroxyapatite at the atomic level. *Clin. Orthop.* 113, 249–262.
- Zahradnik, R.T., Moreno, E.C., Burke, E.J., 1976. Effect of salivary pellicle on enamel subsurface demineralization *in vitro*. *J. Dent. Res.* 55, 664–670.
- Zhang, J., Nancollas, G.H., 1991. Dissolution kinetics of calcium phosphates involved in biomineralization. In: Garside, J., Davey, R.J., Jones, A.G. (Eds.), *Advances in Industrial Crystallization*. Butterworth-Heinemann, Oxford, pp. 47–62.
- Ziegler, A., Hagedorn, M., Ahearn, G.A., Carefoot, T.H., 2007. Calcium translocations during the moulting cycle of the semiterrestrial isopod *Ligia hawaiiensis* (Oniscidea, Crustacea). *J. Comp. Physiol. B* 177, 99–108.
- Ziegler, A., Miller, B., 1997. Ultrastructure of CaCO<sub>3</sub> deposits of terrestrial isopods (Crustacea, Oniscidea). *Zoomorphology* 117, 181–187.
- Ziegler, A., Weihrauch, D., Hagedorn, M., Towle, D., Blecher, R., 2004a. Expression and polarity reversal of V-type H<sup>+</sup>-ATPase during the mineralization-demineralization cycle in *Porcellio scaber* sternal epithelial cells. *J. Exp. Biol.* 207, 1749–1756.
- Ziegler, A., Weihrauch, D., Hagedorn, M., Towle, D.W., Blecher, R., 2004b. Expression and polarity reversal of V-type H<sup>+</sup>-ATPase during the mineralization-demineralization cycle in *Porcellio scaber* sternal epithelial cells. *J. Exp. Biol.* 207, 1749–1756.
- Zundelevich, A., Lazar, B., Ilan, M., 2007. Chemical versus mechanical bioerosion of coral reefs by boring sponges—lessons from *Pione cf. vastifica*. *J. Exp. Biol.* 210, 91–96.